

ADSORPTION OF HEXAHYDRO-1,3,5-TRINITRO-1,3,5-TRIAZINA (RDX) ON SOIL AND CLAY MINERAL SURFACES

by

Wilman Cabrera Lafaurie

A thesis submitted in partial fulfillment of the requirements for the degree of

**MASTER OF SCIENCE
in
CHEMISTRY**

UNIVERSITY OF PUERTO RICO
MAYAGÜEZ CAMPUS
2008

Approved by:

Samuel P. Hernández-Rivera, PhD
Member, Graduate Committee

Date

Miguel A. Muñoz, PhD
Member, Graduate Committee

Date

Nairmen Mina, PhD
President, Graduate Committee

Date

Jaime Benítez, PhD
Representative of Graduate Studies

Date

Francis Patrón, PhD
Chairperson of the Department

Date

ABSTRACT

Hexahydro-1,3,5-trinitro-1,3,5-triazine (RDX) is an energetic compound that is commonly used as a military explosive. Studies indicate that nitroamines compounds, particularly those exhibiting several NO_2 groups or other electron-withdrawing substituents, may adsorb strongly and reversibly from aqueous solutions to natural clay minerals. To determine the fate and transport mechanisms of explosives contained on buried landmines it is essential to understand the adsorption process on soil and clay minerals. In this research, the adsorption behavior of RDX was evaluated in soil samples and clay fractions from the Ap, and A horizons of the Jobos Series at Isabela, Puerto Rico and the University of Puerto Rico Mayaguez (UPRM campus). The clay fraction was separated from the other soil components by centrifugation. We analyzed the mass of solute sorbed per unit mass of soil at equilibrium ($\mu\text{g/g}$) and the aqueous equilibrium phase solute concentration (L/kg) using high-performance liquid chromatography (HPLC). Adsorption coefficients (K_d) for the RDX-soil and RDX-clay interaction were determined. The adsorption process for RDX-soil was described by the Freundlich model. The higher adsorption coefficient was observed in the UPRM soil (0.99 L/Kg). The Freundlich algorithm also described the adsorption process for RDX-clay interaction. The relative adsorption capacity of the clays for RDX was higher in the A horizon (4.42 L/Kg). These results suggest that adsorption by soil organic matter predominates over adsorption on clay minerals when significant soil organic matter content is present. It was also found that properties like cation exchange capacity, surface area, type of exchangeable cations and clay minerals present in the clay fractions are important factors in the adsorption of RDX on clay and soils. The experimental adsorption enthalpy ($\Delta H_{\text{ads}} = -18.46 \text{ KJ/mol}$) found for the RDX-soil interaction, suggests that these interactions are of the Van der Waals type.

RESUMEN

Hexahydro-1,3,5-trinitro-1,3,5-triazina (RDX) es un compuesto energético que se usa generalmente como explosivo militar. Los estudios indican que compuestos como las nitroaminas, particularmente las que exhiben varios grupos NO_2 , pueden fijarse por adsorción fuertemente y reversiblemente en soluciones acuosas sobre minerales de arcilla. Para determinar el destino y el mecanismo de transporte de los explosivos contenidos en minas terrestres es esencial entender el proceso de la adsorción en el suelo y los minerales de arcilla. En este estudio, el comportamiento de la adsorción del RDX fue evaluado en muestras de suelo y arcilla de los horizontes Ap y A de la serie Jobos de Isabela, Puerto Rico y una muestra del campus de la universidad de Puerto Rico en Mayaguez (UPRM). La fracción de arcilla fue separada de los otros componentes del suelo por centrifugación. Analizamos la masa del soluto absorbida por la unidad de masa del suelo en el equilibrio ($\mu\text{g/g}$) y la concentración acuosa del soluto de la fase de equilibrio (L/kg) usando cromatografía líquida de alta presión (HPLC). Los coeficientes de adsorción (K_d) para las interacciones de RDX-suelo y RDX-arcilla fueron determinados. El proceso de adsorción de la interacción RDX-suelo fue descrito por el modelo de Freundlich. El coeficiente de adsorción más alto fue observado en el suelo UPRM (0.99 L/Kg). El modelo de Freundlich también describió el proceso de la adsorción para la interacción RDX-arcilla. La capacidad relativa de adsorción más elevada en las interacciones RDX-arcilla se obtuvieron en el horizonte A (4.42 L/Kg). Estos resultados sugieren que el contenido de materia orgánica en las muestras de suelo tiene un efecto importante sobre la adsorción en los minerales de arcilla cuando el contenido de esta es significativo. Se encontró también que características como capacidad de intercambio catiónico, área superficial y el tipo de mineral de arcilla presente en las fracciones de la arcilla son factores importantes en la adsorción del RDX sobre el suelo y la arcilla. También, se determinó experimentalmente la entalpía de adsorción ($\Delta H_{ads} = -18.46 \text{ KJ/mol}$) para la interacción RDX-suelo. Este valor sugiere que las interacciones son del tipo de Van der Waals.

Copyright © by
Wilman Cabrera Lafaurie
2008

*To God, to my parents, brothers,
and wife.*

ACKNOWLEDGMENTS

I am very grateful to those who collaborated with me in one way or another, but especially I want to say thank to you :

Dr. Nairmen Mina thanks for giving me the opportunity to work under your leadership and guidance in this project and for helping me grow up.

Dr. Miguel A. Muñoz thanks for your time, for giving me the opportunity to be part of your graduate team.

Dr. Samuel Hernandez thanks for your collaboration and for being part of my committee.

Leonardo Pacheco, Ricardo Infante, Katherine Quiñones and Emmanuel Feliciano thanks for your unconditional support and your friendship, the world needs more people like you.

My parents, Carmen and Euclides, thanks for all your love and for always believing in me, my success is yours.

My wife, Maryoris Carrillo, thanks for all your love, understanding and unconditional support, I love you baby.

My lab partners, thanks for all the shared moments, you made the lab a comfortable place.

TABLE OF CONTENTS

LIST OF TABLES.....	ix
LIST OF FIGURE	xi
1 INTRODUCTION	1
2 LITERATURE REVIEW	4
3 THEORY OVERVIEW.....	7
3.1 Clay Minerals	7
3.2 Chemical Explosive.....	10
3.2.1 RDX (Hexahidro-1,3,5-Tinitro-1,3,5-Triazine).....	10
3.3 Chromatography	13
3.3.1 High Pressure Liquid Chromatography.....	13
3.3.2 UV-VIS Detector (Variable Wavelength Detector).....	15
3.3.3 HPLC Applications	16
3.4 Adsorption	18
3.4.1 Freundlich Adsorption Model.....	19
3.4.2 Langmuir Adsorption Model.....	20
4 METHODOLOGY	22
4.1 Separation of soil main fractions: sand, silt and clay.....	22
4.1.1 Removal of Carbonates and Organic Matter	22
4.1.2 Clay Separation	22
4.1.3 Sand and Silt Separation	23
4.1.4 Clay Saturation	23
4.1.5 Determination of pH.....	25
4.2 Soil Texture	25
4.2.1 Soil Texture Using Hydrometer.....	25
4.3 Organic Matter Content	26
4.4 Cation Exchange Capacity	27
4.5 Surface Area	28
4.6 X-Ray Diffraction Analysis	29
4.7 Analytical Method: High Performance Liquid Chromatography	29
4.8 Adsorption Studies.....	30
4.8.1 Sorption Kinetics.....	30
4.8.2 Sorption Isotherms.....	30
4.8.3 Experimental Adsorption Enthalpy.....	31
4.9 Acetonitrile Extraction	32
5. RESULTS AND DISCUSSION.....	33
5.1 Soil Description	33
5.1.2 Texture	36
5.2 Cation Exchange Capacity for Soil and Clay Samples	39
5.3 Surface Area Analysis for Soil and Clay Samples	40
5.4 X-Ray Diffraction Analysis for the Clay Fractions.....	41
5.5 Methodology Validation for RDX Adsorption Studies.....	46
5.6 Sorption Kinetics.....	51
5.7 Sorption Isotherms.....	51
5.8 Experimental Adsorption Enthalpy	62

6.	CONCLUSIONS	64
7.	RECOMMENDATIONS	67
8.	REFERENCES	68
APPENDIX A.	ADSORPTION ISOTHERMS AND LINEAR REPRESENTATIONS.....	71

List of Tables

Table	Page
Table 3.1 Physical and chemical properties of RDX.....	12
Table 5.1 Properties of soil samples from Ap, A horizons and UPRM used in RDX adsorption studies.....	38
Table 5.2 Properties of the clay fractions from Ap, A horizons and UPRM used in RDX adsorption studies	40
Table 5.4 Evaluation of the area for RDX peak in aqueous solution at different concentrations: average area, standard deviation, and relative standard deviation.....	48
Table 5.5 Evaluation of retention time for RDX peak in aqueous solution at different concentrations: average retention time, standard deviation and relative standard deviation.....	49
Table 5.6 Summary of regression parameters for RDX adsorption on soil and clay from Ap, A horizons and UPRM	61
 Appendix A	
Table A.1 Experimental results for RDX interaction with soil from UPRM.....	72
Table A.2 RDX concentrations at equilibrium for three replicates, average concentration and standard deviation found for RDX interactions with soil from UPRM.....	73
Table A.3 Adsorption of RDX by soil for three replicates, average adsorption and standard deviation for RDX interactions with soil from UPRM.....	73
Table A.4 Experimental results for RDX interaction with soil from Ap horizon	74
Table A.5 RDX concentrations at equilibrium for three replicates, average concentration and standard deviation for RDX interactions with soil from Ap horizon	75
Table A.6 Adsorption of RDX by soil for three replicates, average adsorption and standard deviation found for RDX interactions with soil from Ap horizon	75
Table A.7 Experimental results for RDX interaction with soil from A horizon	79
Table A.8 RDX concentrations at equilibrium for three replicates, average concentration and standard deviation for RDX interactions with soil from A horizon	80
Table A.9 Adsorption of RDX by soil for three replicates, average adsorption and standard deviation for RDX interactions with soil from A horizon	80
Table A.10 Experimental results for RDX interaction with the clay fraction from A horizon	84

Table A.11 RDX concentrations at equilibrium for three replicates, average concentration and standard deviation for RDX interaction with the clay fraction from A horizon	85
Table A.12 Adsorption of RDX by clay fraction for three replicates, average adsorption and standard deviation for RDX interactions with the clay fraction from A horizon	85
Table B.13 Experimental results for RDX interaction with the clay fraction From Ap horizon	86
Table A.14 RDX concentrations at equilibrium for three replicates, average concentration and standard deviation for RDX interactions with clay fraction from Ap horizon	87
Table A.15 Adsorption of RDX by clay fraction for three replicates, average adsorption and standard deviation for RDX interactions with clay fraction from Ap horizon	87
Table A.16 Experimental results for RDX interaction with the clay fraction from UPRM.....	91
Table A.17 RDX concentrations at equilibrium for three replicates, average concentration and standard deviation found for RDX interactions with clay fraction from UPRM.....	92
Table A.18 Adsorption of RDX by clay fraction for three replicates, average adsorption and standard deviation for RDX interactions with the clay fraction from UPRM.....	92

List of Figures

Figure	Page
Figure 3.1 Examples of clay minerals with expanding and not expanding interlayer sites.....	9
Figure 3.2 RDX molecule (Hexahydro-1,3,5-trinitro-1,3,5-triazine).....	11
Figure 3.3 Schematic representation of an HPLC system.....	15
Figure 3.4 Agilent 1100 series HPLC modules from Agilent technologies system used for RDX adsorption studies.....	18
Figure 4.1 Clay separation: a) centrifuge used to separate the clay fraction and b) collection of the clay suspension.....	24
Figure 4.2 Physical separation of silt and sand: a) sand and silt, b) sand separated by a mesh sieve and c) silt aqueous solution.....	24
Figure 5.1 Soil profile for Jobos Series showing the distinctive horizontal layers.....	34
Figure 5.2 USDA Textural Triangle.....	38
Figure 5.3 Structural diagram for Kaolinite showing the hydroxyl and siloxane Surface.....	42
Figure 5.4 X-ray diffraction mineral characterization of the clay fraction from A horizon	43
Figure 5.5 X-ray diffraction mineral characterization of the clay fraction from Ap horizon.....	44
Figure 5.6 X-ray diffraction mineral characterization of the clay fraction from UPRM	45
Figure 5.7 Chromatogram for 12 ppm RDX aqueous solution.....	47
Figure 5.8 Calibration curve for RDX in aqueous solution: Average Area vs. Concentration.....	50
Figure 5.9 kinetics of adsorption of RDX on soil and clay Ap horizon.....	53
Figure 5.10 Adsorption isotherm for RDX on soil from UPRM.....	54
Figure 5.11 Freundlich linear representation for RDX adsorption on soil From UPRM	55
Figure 5.12 Langmuir linear representation for TNT adsorption on soil from UPRM.....	56
Figure 5.13 Adsorption isotherm for RDX on clay fraction from A horizon.....	58
Figure 5.14 Langmuir linear representation for RDX adsorption on clay Fraction from A horizon.....	59
Figure 5.15 Freundlich linear representation for RDX adsorption on clay fraction from A horizon.....	60
Figure 5.16 Temperature dependence of Kd of RDX.....	63

Appendix A

Figure A.1 Adsorption isotherm for RDX on soil from Ap horizon.....	76
Figure A.2 Langmuir linear representation for RDX adsorption on soil from Ap horizon	77
Figure A.3 Freundlich linear representation for RDX adsorption on soil from Ap horizon	78
Figure A.4 Adsorption isotherm for RDX on soil from A horizon	81
Figure A.5 Langmuir linear representation for RDX adsorption on soil from A horizon	82
Figure A.6 Freundlich linear representation for RDX adsorption on soil from A horizon	83
Figure A.7 Adsorption isotherm for RDX on clay from Ap horizon	88
Figure A.8 Langmuir linear representation for RDX adsorption on clay from Ap horizon	89
Figure A.9 Freundlich linear representation for RDX adsorption on clay from Ap horizon	90
Figure A.10 Adsorption isotherm for RDX on clay from UPRM	93
Figure A.11 Freundlich linear representation for RDX adsorption on clay from UPRM.....	94
Figure A.12 Langmuir linear representation for RDX adsorption on clay from UPRM	95

1 INTRODUCTION

Hexahydro-1,3,5-trinitro-1,3,5-triazine (RDX) is an energetic compound that is commonly used as a military explosive. Various commercial and military activities that include manufacturing, waste discharge, testing and training, demilitarization, and open burning/open detonation (OB/OD) have resulted in extensive RDX contamination of soil and groundwater ⁽¹⁾. The toxicity of RDX to humans and mammals is well established. RDX is classified as a Class C (possible human) carcinogen, and can cause unconsciousness and epileptiform seizures. RDX is also used as a rodenticide, and the Surgeon General recommends a 24-h maximum RDX concentration of 0.3 mg l⁻¹ to protect aquatic life. In the U.S., the Office of Drinking Water has set a limit for lifetime exposure to RDX at 0.1 mg l⁻¹ ⁽²⁾. The understanding of the interaction of this explosive and its degradation products in soil and soil components could help to detect their presence and determine optimum conditions for its detection.

The nitroamine explosive has low octanol-water partition coefficients (values for RDX of 0.87) and, subsequently, a high potential for mobility in the environment. The sorption characteristics of RDX to specific soil components have not been extensively investigated, although RDX has been shown to exhibit a low sorption coefficient in top soil and to be relatively unaffected by the exchangeable-cation composition during adsorption to clay minerals ⁽³⁾.

Soils are composed of four main fractions: mineral material, organic material, air and water. A typical soil consists of about 45% mineral material,

~5% organics, and ~50% air and water ⁽⁴⁾. The type of soil that occurs in an area is determined by factors such as climate, biota, topography, parent material, and time. Each soil can be characterized and classified based on its texture, color, percent organic matter, effervescence, pH, and structure ⁽⁴⁾.

To understand the adsorption mechanism between RDX and the soil components we determined soil texture in a quantitative way. Soil texture is a term commonly used to designate the size distribution of mineral particles in a soil. These particles fit within definite sizes limits: sand (2.0 – 0.05 mm), silt (0.05 – 0.002 mm) and clay (< 0.002 mm) ⁽⁴⁾. Each fraction possesses different physical characteristics and the nature of the soil will be determined by the particular separate that is present in larger amounts. Thus, a soil possessing a large amount of clay has quite different physical properties from one made up mostly of sand and silt. These three separates play an important role in soil environments, but the clay fraction has the greatest influence on soil physical and chemical properties ⁽⁵⁾.

In this work we present the extraction of clay minerals from soil samples using the mechanical analysis method and the determination of soil texture using the hydrometer method. Physical and chemical studies such as cation exchange capacity (CEC), surface area, percentage of organic matter, pH and x-ray diffraction analysis are also included in this work. RDX adsorption studies for soil and clay samples were done using High Performance Liquid Chromatography (HPLC). This chromatographic technique coupled with Variable Wavelength

Detector (VWD) with Deuterium Lamp, detector provides both qualitative and quantitative information necessary for the identification and quantification of RDX and its degradation products in soil.

2. LITERATURE REVIEW

During the past few years, researchers have dedicated part of their time and efforts to study the behavior of nitroamines on clay mineral surfaces. They developed adsorption methods in which they put in contact aqueous solutions of nitro-compounds, like RDX and TNT, with solid surfaces of clay minerals.

In 1993, Stefan B. Haderlein and René P. Schwarzenbach ⁽⁶⁾ studied the sorption of a series of substituted nitrobenzenes and nitrophenols on homoionic kaolinite. This clay mineral has different surface sites that are representative of many minerals. Using sorption experiments and then analyzing the equilibrium liquid-phase by reverse phase HPLC (High Performance Liquid Chromatography) they found that the strength of the adsorption depends on the structure of the compound and in the type of cation adsorbed on the siloxane surface.

In 1998, J Singh, S.D. Comfort, L.S. Hundai and P.J. Shea ⁽⁷⁾ characterized RDX sorption and long-term fate to predict RDX availability and develop remediation strategies. They characterized RDX sorption and availability in Sharpsbur surface soil by equilibrating the soil with 32 mg RDX L⁻¹ for 168 days; similar experiments were performed with contaminated and uncontaminated subsurface soil. Their experiment indicated limited RDX sorption transformation in the Sharpburg surface and subsurface soils. Most of the sorbed ¹⁴C was potentially available for transport, indicating the importance of remediating RDX contaminated soil to protect groundwater quality.

In 2001, T. W. Sheremata and coworkers ⁽¹⁾ studied the adsorption-desorption behavior and long-term fate of RDX on sterile and nonsterile topsoil. They used reverse phase high-pressure liquid chromatography to determine the concentrations of RDX adsorbed on topsoil, in which sand was the predominant component. The results revealed that the adsorption capacity constant for RDX is considerably less than ($K_d = 0.83$ L/kg) those of 2,4,6-trinitrotoluene and its two metabolites for the same topsoil ($K_d = 6.38 - 11.96$ L/kg). Similar quantities of RDX were recovered on both sterilized and nonsterilized systems during the first week. For the next five weeks a high percent of recovery for RDX was found on sterile topsoil but it completely disappeared in nonsterile topsoil, only metabolites like MNX were formed.

In 2003, Deborah R. Felt, Steven L. Larson, Altaf Wani, and Jeffrey L. Davis ⁽⁸⁾ analyzed products of degradation of RDX in environmental samples. They observed that the nature of the metabolites and breakdown products depends on the treatment process or the weathering that the sample has undergone. McCormick⁽⁹⁾ identified hexahydro-1-nitroso-3,5-dinitro-1,3,5-triazine (MNX), hexahydro-1,3-dinitroso-5-nitro-1,3,5-triazine (DNX), hexahydro-1,3,5-trinitroso-1,3,5-triazine (TNX) as products of sequential reduction of RDX.

In 2004 Hatzinger Paul B, Fuller Mark E, Rungmakol Darin, Schuster Rachel L., and Steffan, Robert ⁽¹⁰⁾ studied the adsorption and desorption isotherms for 2,4,6-trinitrotoluene (TNT), hexahydro-1,3,5-trinitro-

1,3,5-triazine (RDX), and octahydro-1,3,5,7-tetranitro-1,3,5,7-tetrazocine with a wide variety of natural and man-made adsorbents, including wheat straw, sawdust, peat moss, ground rubber tires, and clays. Among the various adsorbents tested, peat moss proved to be the most effective sorbent for the three explosives. The adsorption coefficients (K_d) for TNT and RDX with peat (310 and 87 L/kg, respectively) were at least two orders of magnitude higher than that determined for adsorption of these energetics compounds with two surface soils.

3. THEORY OVERVIEW

3.1 Clay Minerals

Clay minerals are hydrous aluminium phyllosilicates, sometimes with variable amounts of iron, magnesium, alkali metals, alkaline earths and other cations. Clays have structures similar to the micas and therefore form flat hexagonal sheets. Clay minerals are common weathering products (including weathering of feldspar) and low temperature hydrothermal alteration products.

Like all phyllosilicates, clay minerals are characterized by two-dimensional sheets of corner sharing SiO_4 and AlO_4 tetrahedra. Each tetrahedron shares 3 of its vertex oxygen atoms with other tetrahedra. The fourth vertex is not shared with another tetrahedron and all of the tetrahedra "point" in the same direction. These tetrahedral sheets have the chemical composition $(\text{Al},\text{Si})_3\text{O}_4$. According to the arrangement of tetrahedral and octahedral sheets, clay minerals can be classify into two groups, 1:1 and 2:1 type minerals.

The 1:1 layer minerals contain one tetrahedral and one octahedral sheet in their basic structural unit. This type of mineral is represented by the kaolin group with the general formula $\text{Al}_2\text{Si}_2\text{O}_5(\text{OH})_4$. The most common mineral in this group is Kaolinite. It is particularly abundant in more weathered soils such as Udisols and Oxisols. Kaolinite has very little isomorphous substitution in its octahedral and tetrahedral sheets, which results in very little or no permanent

charge. Therefore, if we compare Kaolinite with others clay minerals, its cation exchange capacity and surface area are considered lower.

In 2:1 minerals, an octahedral sheet is bonded to two tetrahedral sheets. The octahedral sheet is generally between the two tetrahedral sheets. This group of minerals is represented by the mica, smectite, and vermiculite groups. Depending on the degree of charge due to isomorphous substitution, some of these clay minerals have the ability to expand their interlayer sites between two 2:1 layers (See figure 3.1). This provides high surface area and adsorptive properties which could help in the remediation of organic and inorganic pollutants, enhancing their degradation and attenuating their movement.

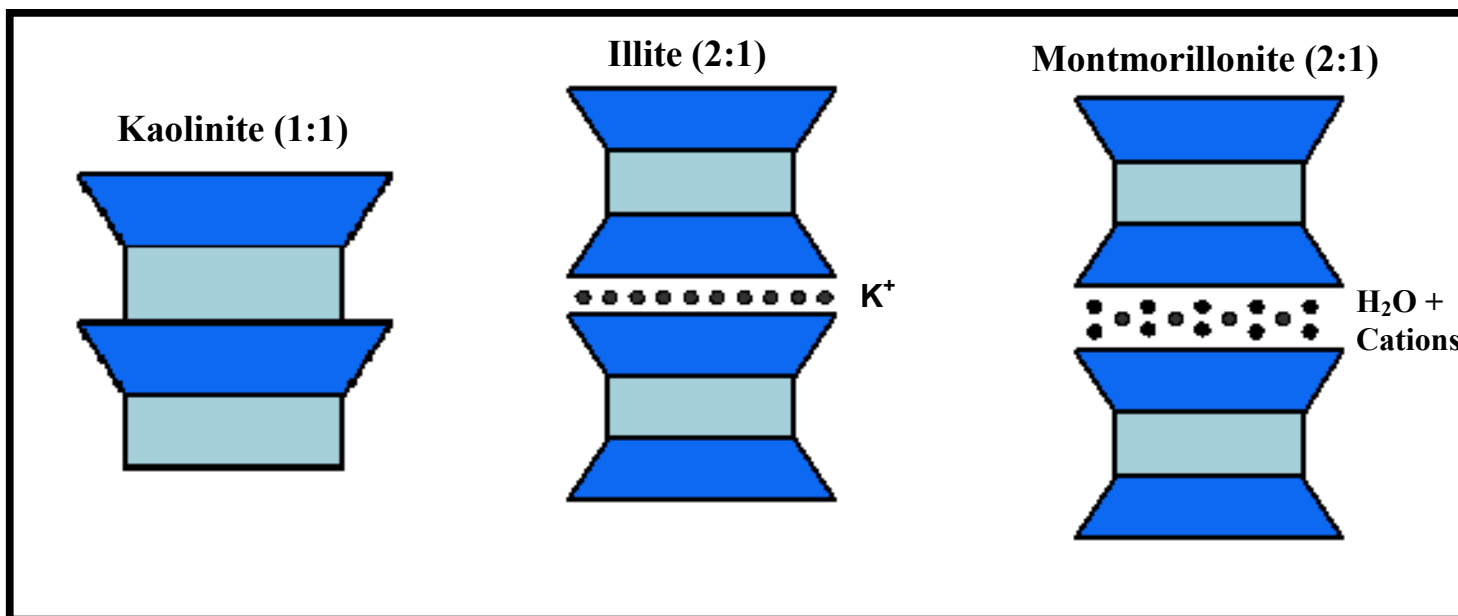


Figure 3.1 Examples of clay minerals with expanding and not expanding interlay

From: G. N. White and J. B. Dixon, *Soil Mineralogy with Environmental Applications*, SSSA Book Series No. 7, Chapter 12, Soil Science of America, Inc., Madison, Wisconsin, 2002.

3.2 Chemical Explosive

An explosive is a material, either a single substance or a mixture of substances, which is capable of producing an explosion by its energy released on detonation. The explosives can be classified in three categories: propellants, primary or low explosives and secondary or high explosives.

The propellants are combustible materials and do not detonate as their principal reaction, but rather deflagrate. Primary explosives or initiators can be easily detonated when they are heated or subjected to shock or spark. Finally, high or secondary explosives detonate under the influence of the shock wave of explosion of a suitable primary explosive ⁽¹¹⁾. The explosive studied in this investigation, RDX, is a secondary explosive.

3.2.1 RDX (Hexahydro-1,3,5-trinitro-1,3,5-triazine)

The discovery of RDX dates from 1899 when Hans Henning obtained a German patent for its manufacture, by nitrating hexamethylenetetramine nitrate⁽¹²⁾ (figure 3.2).

RDX is a white, crystalline solid with a melting temperature of 204 °C. Some advantages of RDX include its low cost, safety in handling, fairly high explosive power, good chemical and thermal stability, compatibility with other explosives, and a low melting point favorable for melt casting operations. On the other hand, this explosive is considered toxic. Some manifestation of RDX

absorption include: aplastic anemia, toxic jaundice, cyanosis, gastritis and dermatitis. Some of the properties of RDX are presented in Table 3.1.

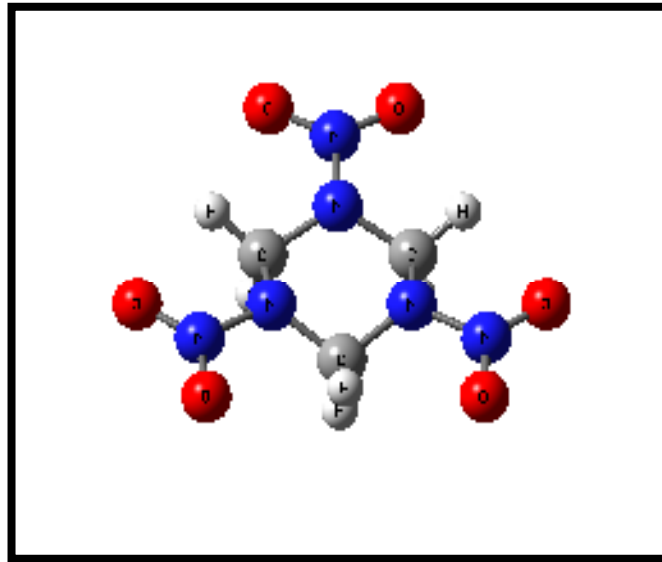


Figure 3.2 RDX (Hexahydro-1,3,5-trinitro-1,3,5-triazine)

Table 3.1 Physical and chemical properties of RDX

Physical and Chemical Properties of Hexahydro-1,3,5-trinitro-1,3,5-triazine (RDX)	
Molecular Weight	222.12 g/mol
Molecular Formula	$C_3H_6N_6O_6$
Density	1.82 g/cm ³
Solubility in water at 25 °C	Low
Melting Point	205.5 °C
Vapor Pressure	4.6×10^{-6} torr
Ignition Point	225 °C

Hatzinger et al (2004)

3.3 Chromatography

The distribution of analytes between phases can often be described quite simply⁽¹³⁾. An analyte is in equilibrium between the two phases:



The equilibrium constant K for this reaction is called a partition ratio, or partition coefficient, and is defined as:

$$K = \frac{C_S}{C_M} \quad [3.2]$$

where C_S is the molar analytical concentration of the solute in the stationary phase and C_M is its analytical concentration in the mobile phase.

3.3.1 High Performance Liquid Chromatography

High-performance liquid chromatography (HPLC) is a form of column chromatography used frequently in analytical chemistry. HPLC is used to separate components of a mixture by using a variety of chemical interactions between the substance being analyzed (analyte) and the chromatography column. Two types of partition chromatography are distinguishable based upon the relative polarities of the mobile and stationary phases⁽¹⁴⁾.

These two types of partition chromatography are: normal-phase and reverse phase.

In normal-phase a relatively nonpolar solvent served as the mobile phase and polar supports as stationary phase. Here, the least polar component is eluted first because it is the most soluble in the mobile phase. In contrast, reverse-phase used a nonpolar stationary phase (often a hydrocarbon) and a relatively polar mobile phase (such as water, methanol, or acetonitrile). In reverse-phase method, the most polar component appears first, and increasing the mobile phase polarity increases the elution time.

The basic operating principle of HPLC (Figure 3.3) is to force the analyte through a column of the stationary phase (usually a tube packed with small spherical particles with a certain surface chemistry) by pumping a liquid (mobile phase) at high pressure through the column. The sample to be analyzed is introduced in small volume to the stream of mobile phase and is retarded by specific chemical or physical interactions with the stationary phase as it traverses the length of the column. The amount of retardation depends on the nature of the analyte, stationary phase and mobile phase composition. The time at which a specific analyte elutes (comes out of the end of the column) is called the retention time and is considered a reasonably unique identifying characteristic of a given analyte. The use of pressure increases the linear velocity (speed) giving the components less time to diffuse within the column, leading to improved resolution in the resulting chromatogram.

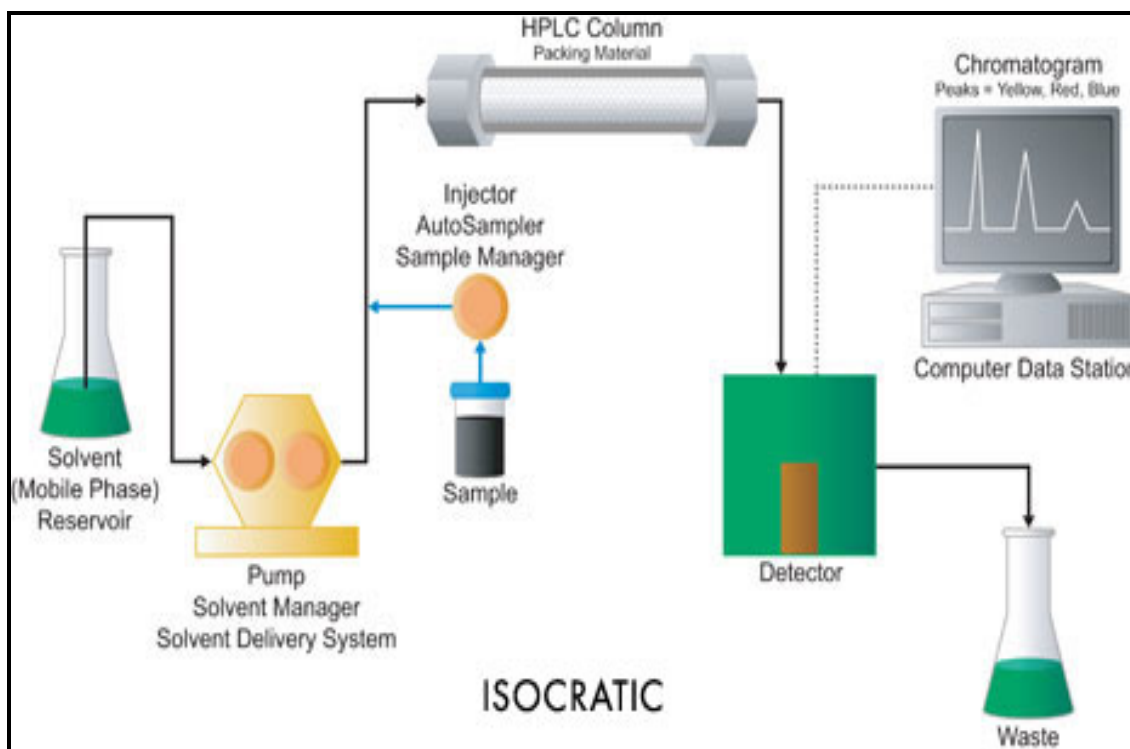


Figure 3.3 Schematic representation of an HPLC system.

From: <http://www.waterscorporation.com> (© 2008 Waters Corporation)

3.2.2 UV-VIS Detector (Variable Wavelength Detector).

UV detector is the most used in HPLC. The cell volume is 1 to 10 μL and the optical pathlength is 2 to 10 nm. The detector measures the concentration of sample bands as they leave the column and pass through the detector flow cell. When no band is passing through the detector, a constant signal is recorded called the baseline of the chromatogram or detector. When a sample band reaches the detector, the detector responds to the difference in the mobile phase properties caused by the presence of the sample compound, giving rise to a change in detector signal, seen as a peak. A photometric detector, in its simplest form, consists of a light source, a flow cell (or "sample cell"), and a light sensor.

The signal displayed increases in proportion to the concentration of sample in the flow cell. The detector will also respond to other changes in the contents of the flow cell. The detector wavelength is an important characteristic of an HPLC separation.

As a general rule, the wavelength is set to the absorbance maximum of the analyte. Using the wrong wavelength may result in decreased peak heights, or even no peaks at all. Because different compounds can have different absorbance spectra, a direct quantitative comparison of different peaks in the same chromatogram can be misleading. A small quantity of a compound which absorbs strongly at the detector wavelength can give a bigger peak than a large quantity of a weak absorber. For reliable quantification, a calibration must be carried out with a known quantity of the exact compound to be analyzed ⁽¹⁵⁾.

3.3.3 HPLC Applications

High-performance liquid chromatography is the most widely used of all of the analytical separation techniques. The reasons for the popularity of the method are its sensitivity, its ready adaptability to accurate quantitative determinations, and its suitability for separating nonvolatile species or thermally fragile ones. Also, its widespread applicability to substances that are of prime interest to industry, to many fields of science. These characteristics make HPLC one of the most used separation techniques. During the last 10 years HPLC has

gained popularity in the analysis of explosives and their degradation products in various matrices such as pharmaceutical formulations, water, soil and air ⁽¹⁴⁾. Most of the separations involving explosives of the same chemical class were isocratic runs with simple methanol-water or acetonitrile–water mixtures as mobile phases. Gradient and flow programs were applied only when the analysis involved a mixture of explosives of different chemical classes. Several RP-8 and RP-18 columns were used with particle sizes of 5, 7 and 10 μm .

For RDX adsorption studies presented in this research we used a Agilent 1100 Series HPLC modules from Agilent Technologies (figure 3.4), Inc., Palo Alto, a Variable Wavelength Detector (VWD) with Deuterium Lamp and a temperature control module. Separation was performed with a Zorbax Eclipse XDB Column C18 (4.6 X 150 mm, 5 μm) from Agilent maintained at 40 °C. The explosives were separated by means of reversed-phase LC, and gradient mobile phase (50-50% water, methanol) was used at a flow of 1.00 mL/min.

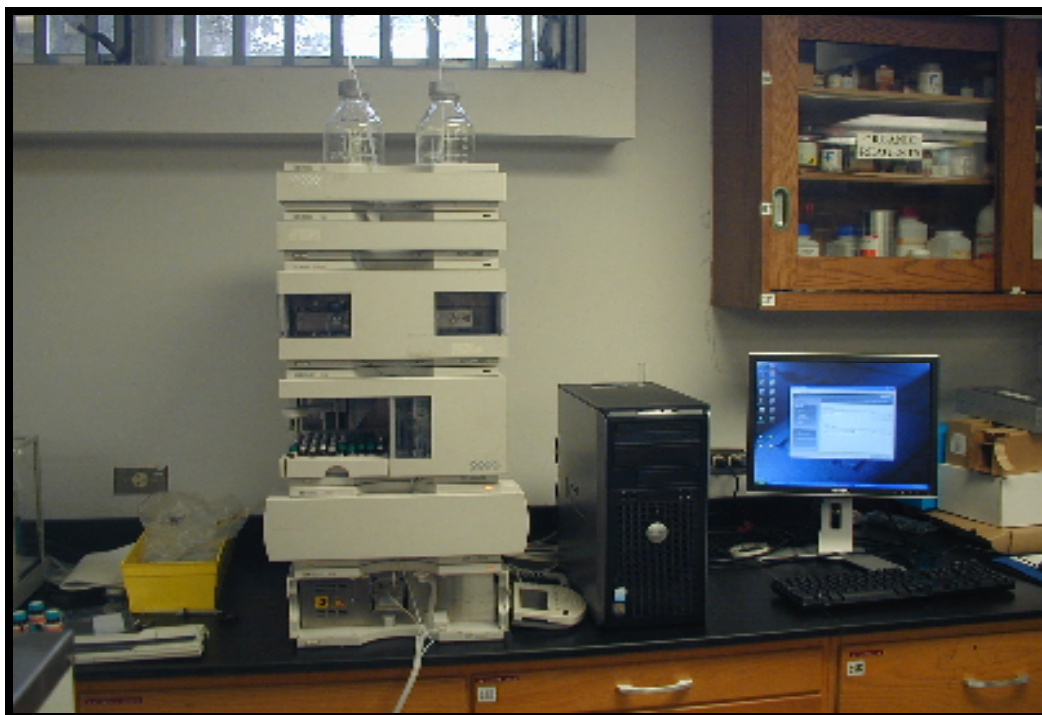


Figure 3.4. Agilent 1100 Series HPLC modules from Agilent Technologies system used for RDX adsorption studies.

3.4 Adsorption

Adsorption is the accumulation of atoms, molecules, or ions at the surface of a solid or liquid as the result of physical or chemical forces. It differs from absorption, in that an adsorbed substance remains at the surface while an absorbed substance spreads throughout the absorbing material. An adsorbed substance is termed an adsorbate while the material on which adsorption occurs is the substrate. The release of an adsorbate is termed desorption. Adsorption is usually described through isotherms, that is, functions which connect the amount of adsorbate on the adsorbent, with its pressure (if gas) or concentration (if liquid). The most widely used adsorption isotherm equation employs a simple

linear function. An adsorption isotherm equation is conveniently expressed in terms of the distribution coefficient, K_d :

$$x = K_d C \quad [3.3]$$

where x is the amount of ion adsorbed per unit mass and C is the equilibrium solution ion concentration.

3.4.1 Freundlich Adsorption Model

The most popular adsorption model for a single solute system, the Freundlich model, is an empirical equation based on the distribution of solute between the solid phase and aqueous phase at equilibrium. The basic Freundlich equation is:

$$q = K_d C^{\frac{1}{n}} \quad [3.4]$$

where q describes the mass of adsorbate adsorbed per unit of sorbent, C is the concentration in equilibrium between the adsorbed mass and the media where the process takes place and K_d and $1/n$ are empirical constants. The logarithmic expression of this equation gives a linear relation which allows the determination of some characteristics of the adsorption process.

$$\log q = \log K_d + \frac{1}{n} \log C \quad [3.5]$$

Here, $1/n$ (the slope) define the affinity and K_d (the intercept) define the relative adsorption capacity.

3.4.2 Langmuir Adsorption Model

The Langmuir isotherm or Langmuir adsorption equation relates the coverage or adsorption of molecules on a solid surface to gas pressure or concentration of a medium above the solid surface at a fixed temperature. The equation was developed by Irving Langmuir in 1916. The equation is stated as:

$$\frac{x}{m} = \frac{KCb}{1 + KC} \quad [3.6]$$

where $\frac{x}{m}$ describes the mass of adsorbate adsorbed per unit of sorbent and C is the concentration in equilibrium between the adsorbed mass and the media where the process takes place. In this equation K and b are empirical constants. To describe the adsorption characteristics of the process the linear form of the Langmuir equation is used:

$$\frac{C}{x/m} = \frac{1}{K} + \frac{1}{b} C \quad [3.7]$$

Here, the value of $1/b$ (the slope), where b represents the maximum adsorption of the system and $\frac{1}{K}$ (the intercept) define the value of K which represents the retention energy.

4. METHODOLOGY

4.1 Separation of soil main fractions: sand, silt and clay

4.1.1 Removal of Carbonates and Organic Matter

Soil samples from Ap and A horizons of Jobos soil and the University of Puerto Rico at Mayagüez campus, were obtained down to a depth of 0 to 10 inches in the Jobos Series at Isabela, P.R. The soil was allowed to dry at room temperature, ground and passed through a mesh sieve number 10 of 2 mm opening to ensure an uniform particle size sample. Then, forty grams of soil samples from each soil were placed in 1000 mL beakers and treated with increments of 1N NaOAc to remove carbonates. To remove organic matter the samples were placed in a water bath at 80.0 °C and treated with increments of 5 mL of 30% H₂O₂. These soil samples were free of organic matter. This was indicated by the lack of effervescence.

4.1.2 Clay Separation

The soil samples were transferred to a 250 mL centrifuge tubes using 100 mL of 0.25 M NaCl prepared solution (preliminary disperse solution that helps in the precipitation of clay). The samples were centrifuged in an IEC Model CU-5000 Centrifuge for five minutes at 2000 rpm. All liquid suspension, which may contain excess of H₂O₂ and any remaining organic matter, was poured off. A 0.01 M Na₂CO₃ dispersing solution was used to aid in the transfer of the soil to a mixer. The soil was carefully mixed for approximately 15 minutes at medium-high velocity and then transferred to a 250 mL centrifuge bottles in approximately

equal amounts. Using the dispersing solution; the bottles were filled up to 2 cm from the edge, centrifuged for three minutes at 750 rpm and then pour the clay suspension in a 1000 mL beaker since the specified parameters and gravity will maintain the sand and silt compress at the bottom of the centrifuge bottles (Figure 4.1 b). This step was done several times until the clay suspension came out clear. This was the indication that no apparent clay was remaining. The beakers were left undisturbed until all the suspended clay settled. By means of a siphon the excess disperse solution was poured out.

4.1.3 Sand and Silt Separation

The centrifuged bottle containing the sand and silt was filled with distilled water, shaken and passed through a mesh sieve number 325 to separate the sand fraction. The sand particles stay in the sieve while silt particles were collected in a 1000 ml beaker and left to settle a few weeks prior to removing the excess of water (See figure 4.2 b). The sand and silt fractions were dried at 100 °C for 48 hours and the weight recorded.

4.1.4 Clay Saturation

Saturation of clay colloids with K^+ was needed for analysis like CEC, surface area, and x-ray diffraction. The clay was transferred to a 250 mL centrifuge bottle using no more than 100 ml of 0.1 M KCl solution. This solution was shaken and then centrifuged at 2500 rpm for 5 min and the supernatant removed. The process was repeated two more times and the excess of KCl

solution was washed with three portions of 100 mL distilled water. To the wash of KCl excess, the chlorine test with AgNO_3 was performed. As soon as the centrifugation process ended an aliquot of the supernatant was taken. If no turbidity was observed when AgNO_3 was added, it was assumed that the sample was free of salt.

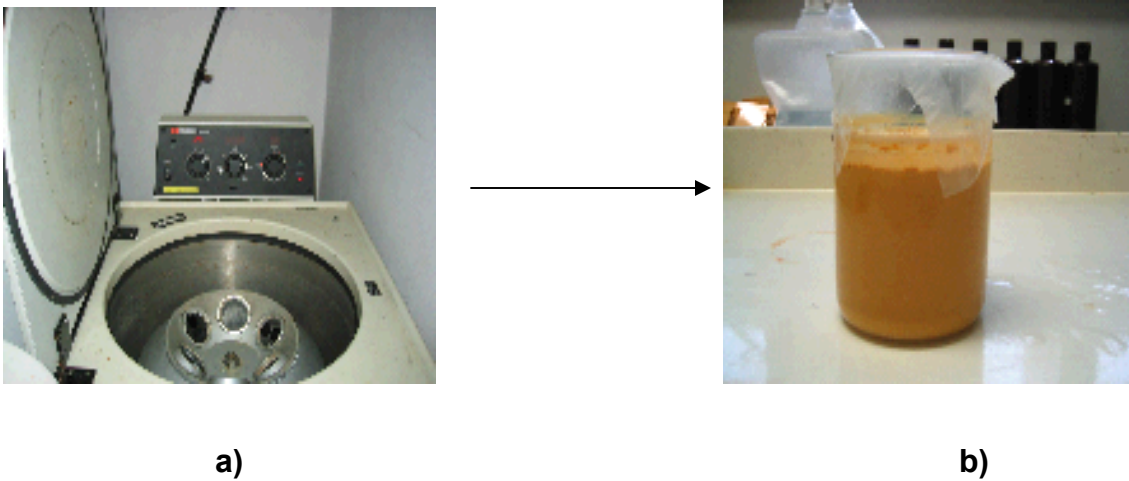


Figure 4.1 Clay separation: a) centrifuge used to separate the clay fraction and b) collection of the clay suspension.

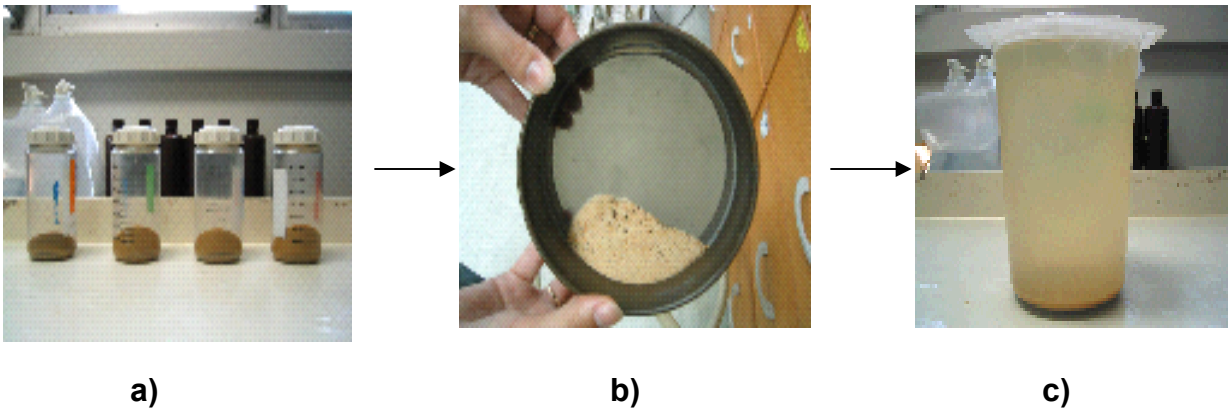


Figure 4.2 Physical separation of silt and sand: a) sand and silt, b) sand separated by a mesh sieve and c) silt aqueous solution.

4.1.5 Determination of pH

To determine the soil pH, soil samples were mixed with distilled water in a proportion of 1:2. For the adsorption studies, it was necessary to adjust the pH of the clay fractions by the addition of diluted HCl solution. All the pH measurements were obtained using a Beckman pH meter model phi 50. After this, clay samples were dried using the freeze-drying technique. This technique minimizes the possibility of structural changes in clay minerals that could be caused by oven-drying.

4.2 Soil Texture

The textural class names of soils was are determined according to the proportion of the different particle size fraction. After a hydrometer method has been completed in the laboratory and the percentage for each soil particle size fraction was calculated, the soil textural class was determined using the USDA textural triangle.

4.2.1 Soil Texture Using Hydrometer

Soil texture was determined using the hydrometer method. First, two soil samples of 50 g were weighed and one of them oven dried at 105 °C in order to determine the soil dry weight. The other soil sample was transferred to a mixer using 200 mL of a sodium metaphosphate solution. This solution containing the soil sample was mixed for 5 minutes and then transferred to a sedimentation cylinder. It was filled to a calibration mark using distilled water and agitated in

upward movement a plunger. The hydrometer was placed into the system and a reading was taken after the first 40 s and the temperature recorded. After this, the hydrometer was taken out and the sodium methaphosphate solution containing the soil sample was agitated again. The reading of the hydrometer and temperature of the system was collected after 2 h. This procedure was performed for the two soil horizons under study.

4.3 Organic Matter Content

The organic matter content was determined for soil samples using the Walkley –Black Method. A soil sample of 0.5 g was transferred into a 500 mL Erlenmeyer flask and 10 mL of 1N $K_2Cr_2O_7$ were added. The flask was swirled gently to disperse the soil in the solution and then 20 mL of concentrated H_2SO_4 were added. Once again, the flask was swirled until soil and reagents were mixed and then the system was undisturbed for about 30 min. After that, 200 mL of distilled water were added to the flask and this suspension was filtered using an acid resistant filter paper. Five drops of *o*-phenanthroline indicator were added and finally the solution was titrated with 0.5 M $FeSO_4$. As the end point is approached, the solution takes on a greenish cast and then changes to dark green and finally to a maroon color. This experiment was performed in duplicate. A blank determination was done in the same manner. Percent of organic matter was calculated from the %Organic Carbon (%OC) as follows:

$$\%OC = \frac{\text{meq } K_2Cr_2O_7 - \text{meq } Fe(NH_4)_2(SO_4)_3}{\text{Soil weight (g)}} \times \frac{0.003 \text{ g of C}}{\text{meq}} \times 100 \quad [4.1]$$

where, 0.003g is the weight of 1 meq of C.

$$\%OM = (\%OC) (1/0.77) (1/0.58) \quad [4.2]$$

where, 0.77 is the %C recovered by the Walkley-Black method, and 0.58 is the conversion factor from carbon to organic matter.

4.4 Cation Exchange Capacity

Displacement of one cation by another results in the process called cation exchange. To determine the cation exchange capacity of the soils under study, 5 g of each soil were placed in 50 mL centrifuge tubes. These tubes were filled with 30 ml of 0.2 M NH_4Cl and then shaken for 5 minutes using a reciprocal shaker. The samples were centrifuged at 2500 rpm for 5 minutes and the supernatant was collected in a 250 ml volumetric flask. This process was repeated four more times and the supernatant added to the 250 mL volumetric flask. The samples previously saturated with 0.2 M NH_4Cl were washed twice with 30 mL deionized water to remove the excess of NH_4Cl . The NH_4^+ adsorbed to exchange sites was extracted using a 0.2 M KNO_3 solution. The samples were washed five times with the 0.2 M KNO_3 solution, centrifuged and the supernatant containing NH_4^+ ions was collected in a 250 mL volumetric flask. The samples were diluted to volume and analyzed using Micro Kjeldahl. The CEC for the clay fraction was determined using the same procedure, but only 2 g of the clay were used.

4.5 Surface Area

For surface area determination 2 g of soil were placed in an aluminum plate and then placed in a furnace at 105 °C for 24 hours. The dry samples were transferred to a CaCl₂ desiccator to prevent moisture absorption during the cooling process. After 15 min the samples were weighed and 3 ml of EGME (Ethylene Glycol Methyl Ether) solution were added. They were placed inside a desiccator equipped with a vacuum outlet and allowed to equilibrate for 30 minutes. A vacuum pump was connected to the desiccator and the samples were evacuated for 45 minutes. Four hours after the evacuation the samples were removed from the desiccator and the weight recorded. The samples were placed again in the desiccator, evacuated and the weight recorded after two hours. This procedure was repeated until constant weight was achieved. This study was performed in duplicate. For clay surface area determination we used a mass of 1g of the clay previously saturated and dried. The surface area was determined using the following equation:

$$SSA = \frac{\text{grams of EGME}}{\text{grams of sample}} \times \frac{1}{2.86 \times 10^{-4} \text{ g/m}^2} \quad [4.3]$$

4.6 X-Ray Diffraction Analysis

Mineral identification in the clay fraction was performed by XRD analysis using a Siemens D5000 unit. This unit consisted of a ceramic Cu tube, graphite monochromator, computer-controlled theta-compensating slit and automated 40

sample changer equipped with the DiffracPlus software and Powder Diffrac File 2002 database. Approximately 1 g of clay from each soil horizon was placed in a sample holder. The scans were collected from 4 to 70 degrees 2-theta, 2 second counts at 0.020 degrees steps. X-Ray analysis was done in the X-Ray Microanalysis Laboratory of the Geology Department of the University of Puerto Rico Mayagüez Campus.

4.7 Analytical Method: High Performance Liquid Chromatography

Chemical analysis was performed by HPLC using a Agilent 1100 Series HPLC modules from Agilent Technologies. The HPLC modules system consisted of a Variable Wavelength Detector (VWD) with Deuterium Lamp and a temperature control module. Separation was performed with a Zorbax Eclipse XDB Column C18 (4.6 X 150 mm, 5 μ m). The methanol/water isocratic mixture was at a flow rate of 1.0 ml/min at a composition of 50:50 was held for 4 minutes. RDX was synthesized and recrystallized to achieve chemical purity of 98.3%. Aqueous RDX solutions were prepared from stock solutions in acetonitrile (0.1 M). A specific volume from stock solution was added to deionized water to give the following initial RDX concentrations 4, 8, 12, 16, 20 and 24 μ g/mL. Acetonitrile concentrations never exceeded 0.5 % (V/V) in the adsorption experiments ⁽¹⁵⁾.

4.8 Adsorption Studies

4.8.1 Sorption Kinetics

RDX stock solution was prepared by dissolving 22.59 mg of RDX (98.3 %) crystalline in 5 mls of acetonitrile. Then a standard RDX aqueous solution of 12 µg/mL was prepared. In 50 mL borosilicate centrifuge tubes, 10 mL of the standard aqueous RDX solutions were combined with 0.2 g of the clay fraction. The background solution for the clay samples was 0.1 M KCl. Centrifuge tubes were wrapped in aluminum foil and agitated on a reciprocal shaker for 1, 4, 8, 28, 48, 54, and 72 hours. After this, the tubes were centrifuged for 3 min at 12000 rpm. The supernatant was filtered using a Millex-HV 0.45 µm filter unit and placed into autosampler vials. The mass of RDX adsorbed by the clay fractions was calculated by difference. For soil adsorption studies the same procedure was done but 2 g of soil were combined with RDX aqueous solution.

4.8.2 Sorption Isotherms

RDX stock solution was prepared by dissolving RDX (98.3%) crystalline in acetonitrile. Dilutions were prepared to make RDX concentrations of 4, 8, 12, 16, 20 and 24 µg/mL in deionized water. In 50 mL borosilicate centrifuge tubes, 10 mL of the aqueous RDX solutions were combined with 0.2 g of the clay fraction. The background solution for the clay samples was 0.1 M KCl. Centrifuge tubes were wrapped in aluminum foil and agitated on a reciprocal shaker for 22 hours. After this, the tubes were centrifuged for 3 min at 12000 rpm. The supernatant was filtered using a Millex-HV 0.45 µm filter unit and placed into autosampler

vials. The mass of RDX adsorbed by the clay fractions was calculated by difference. All experiments were conducted in triplicate. For soil adsorption studies the same procedure was done but 2 g of soil were combined with RDX aqueous solutions without the presence of a background electrolyte. The samples were equilibrated for 22 hours in a reciprocal shaker.

4.8.3 Experimental Adsorption Enthalpy

Adsorption isotherms were measured at different temperatures from 10, 20, 30, 40, 50 and 60 °C. Dilutions were prepared to make RDX concentrations of 4, 8, 12, 16, 20 and 24 µg/mL in deionized water. In 50 mL borosilicate centrifuge tubes, 10 mL of the aqueous RDX solutions were combined with 2 g of the soil. Each sample was vortexed and placed in a sonicator bath for 22 h at the desired temperature. After this, the tubes were centrifuged for 30 min at 3500 rpm. The supernatant was filter using a Millex-HV 0.45 µm filter unit and finally analyzed by HPLC. The adsorption coefficients (K_d) for the different isotherms were determined by modeling the data from the above experiment using the Freundlich equation ⁽⁵⁾. The adsorption enthalpy was determined using the equation of Van't Hoff:

$$\left(\frac{\partial \ln K}{\partial T} \right)_{\ominus} = \frac{\Delta H_{ADS}^{\circ}}{RT^2} \quad [4.4]$$

The linear representation of the van't Hoff equation is:

$$\ln K_d = \frac{\Delta S_{ads}}{R} - \frac{\Delta H_{ads}}{R} \frac{1}{T} \quad [4.5]$$

Therefore, a plot of the natural logarithm of the adsorption coefficients (K_d) versus the reciprocal temperature gives a straight line. The slope of the line is equal to minus the standard enthalpy change divided by the gas constant, $\Delta H^\circ/R$.

4.9 Acetonitrile Extraction

RDX was extracted from the solid phase (soil or clay) using the acetonitrile extraction procedure obtained from EPA SW-846 Method 8330⁽¹⁷⁾. The extraction was conducted by adding 10.0 mL of acetonitrile to the soil pellets for all initial concentrations following adsorption. Each sample was vortexed and placed in a sonicator bath cooled to approximately 22 °C for 18 h. The samples were centrifuged at 3500 rpm for 3 min and 4.0 mL of the supernatant were combined with 4.0 mL of a 5g/L CaCl_2 solution. The solution was agitated and settled for 15 min and then filtered using a Millex-HV 0.45 μm filter unit and finally analyzed by HPLC.

5. RESULTS AND DISCUSSIONS

5.1 Soil Description

The soils used in the study were from the Jobos Series at Isabela, Puerto Rico and a topsoil from the University of Puerto Rico at Mayagüez campus. The Jobos series is a highly weathered soil located at the western region of Puerto Rico. The Soil is classified as Ultisol. This taxonomy order is extensive in Puerto Rico. Ultisols are found primarily in humid temperate and tropical areas, typically on older, stable landscapes. They are strongly leached, with relatively low native fertility. Intense weathering of primary minerals has occurred, and much Ca, Mg, and K has been leached from these soils. Ultisols have a subsurface horizon in which clays have accumulated, often with strong yellowish or reddish colors resulting from the presence of Fe oxides. The soil from Mayaguez Campus is also a highly weathered soil, probably Humatas series.

Soil samples from the Ap and A horizons of Jobos series were selected for the adsorption experiments (See figure 5.1). The A horizon is a surface horizon composed of minerals and organic matter⁽⁴⁾. Plant roots and seeds grow in this horizon. The organic matter is accumulated from growing plants and organic matter decomposed by organisms. The A horizon is the layer of soil at the mineral soil surface, and is roughly equivalent to topsoil. It is usually below the O horizon and above the B horizon. Dark color of the A horizon is due to the mixing of humus with mineral. If the A horizon is more than 2-3 inches thick, it has probably been plowed. It has properties resulting from cultivation, pasturing, or

similar kinds of disturbance under these conditions this horizon is designated as Ap horizon.

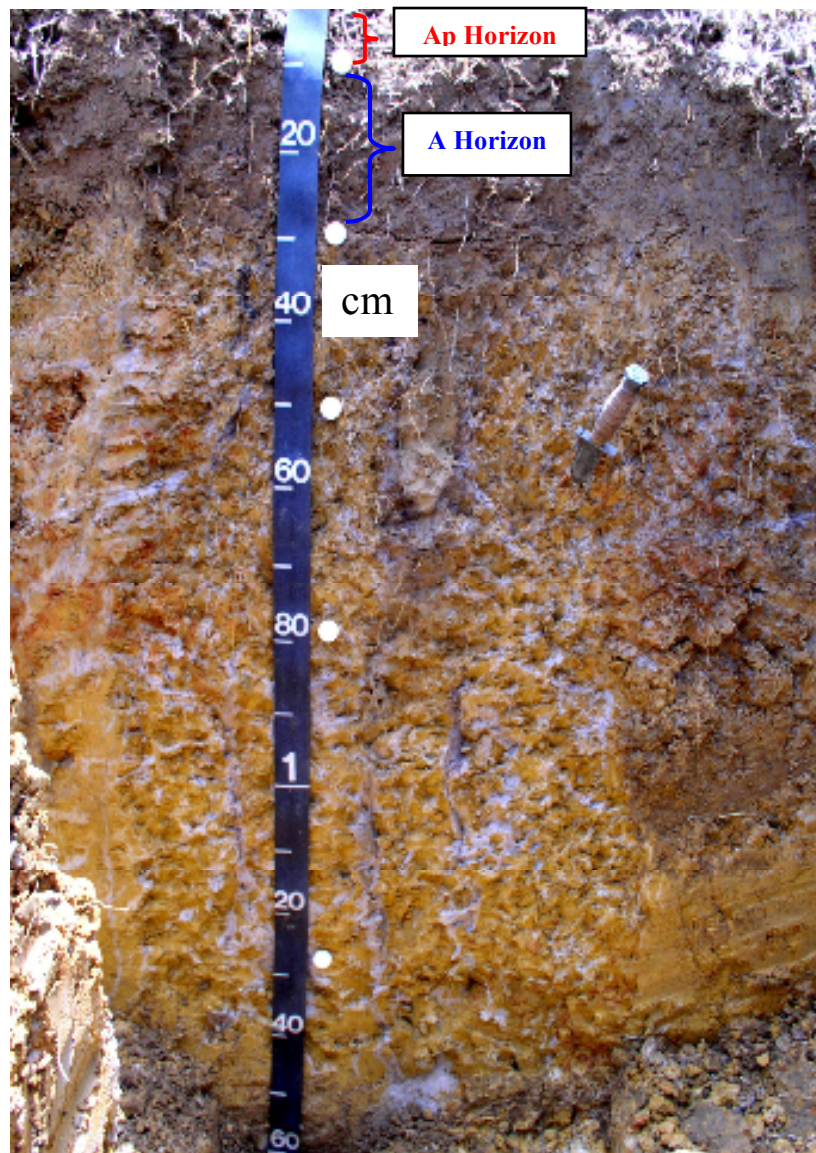


Figure 5.1 Soil profile for Jobos Series showing the distinctive horizontal layers.

The soil from University of Puerto Rico at Mayaguez campus is classified as the Humatas series. The Humatas series consist of very deep, well drained, moderately slowly permeable soils on side slopes and ridges of strongly dissected upland. They forme in clayey and loamy material that weathered from igneous rocks. Is very fine, parasesquic and isohyperthermic typic Haplohumults. The Humatas series is located at the west region of Puerto Rico, approximately 6.5 miles of the city of Mayaguez.

5.1.2 Texture

The use of a hydrometer allowed the determination of soil texture by measuring the grams the soil particles (sand, silt, and, clay) that remain suspended in the cylinder after a specific period of time. Different sized soil particles are separated based on their sedimentation rates. Based on Stokes Law, larger particles will settle faster in a column of water, while smaller particles remain suspended much longer in the solution ⁽⁴⁾. After 40 seconds the largest particles (sand) quickly dropped to the bottom of the cylinder, only silt and clay particles are left suspended in the water. After two hours only clay-sized particles remain suspended.

Table 5.1 shows the distribution of soil separates for the selected soils. A 27.14 % of clay was obtained in Ap horizon, 28.20 % in the A horizon and 53.7% of clay in UPRM soil. According to USDA texture triangle (Figure 5.2), Ap and A horizons are classified as sandy clay loam and UPRM soil is classified as clay. The Ap and A horizons have considerable amounts of sand, which can be most easily detected by moistening the soil and smoothing it out between the fingers. However, as the name implies, sandy clay loam has more clay than the sandy loams and thus possesses greater cohesive properties (such as stickiness and plasticity) when moistened ⁽⁴⁾. **Clay** (UPRM soil): is the finest textured of all the soil classes. Clay usually forms extremely hard clods or lumps when dry and is extremely sticky and plastic when wet. When containing the proper amount of

moisture, it can be "ribboned out" to a remarkable degree by squeezing between thumb and forefinger, and may be rolled into a long, very thin wire ⁽¹⁸⁾.

Table 5.1 Properties of soil samples from Ap, A horizons and UPRM used in RDX adsorption studies.

Horizons	% clay	% silt	% sand	% organic matter	pH	Surface Area (m ² /g)	CEC (meq/100g)
	< 0.002 mm	0.05 – 0.002 mm	0.05 – 2.0 mm				
Ap	27.14	6.26	66.60	6.21	7.52	22.58	3.62
A	28.20	4.09	67.71	4.49	7.09	18.06	2.57
UPRM	53.70	34.12	12.18	1.18	7.05	33.01	6.75

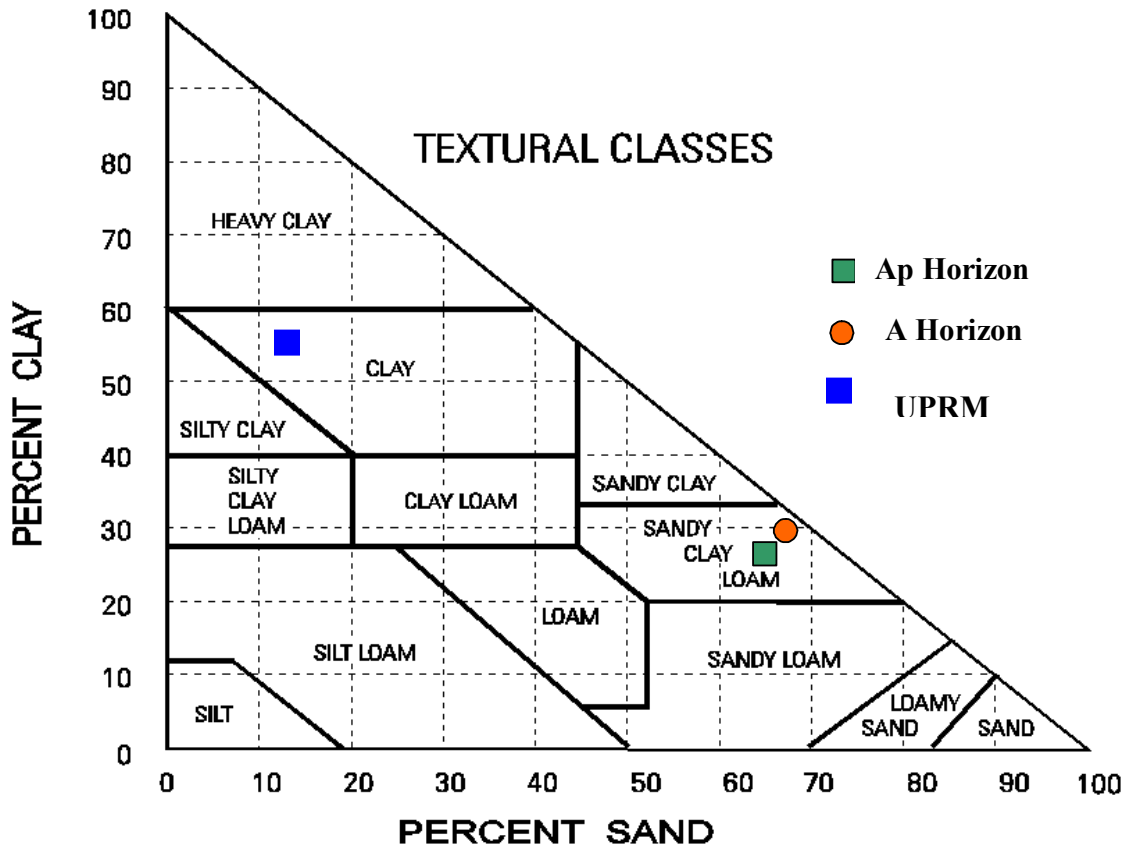


Figure 5.2 USDA Textural Triangle

5.2 Cation Exchange Capacity for Soil and Clay Samples

The cation exchange capacity (CEC) of soils is a measure of the quantity of sites on soil surfaces (primarily clay and organic matter) that can retain positively charged ions by electrostatic forces. The main source of charge on clay minerals is isomorphous substitution; this is the substitution of one element for another in ionic crystals without changes its structure. Charges developed as a result of isomorphous substitution are permanent and not pH dependent. It is important to establish the soil pH because some clay minerals like kaolinite, iron oxides and aluminum oxides present pH dependent charges. This type of charge is variable and negative charges increase with increasing pH. Table 5.1 presents pH and CEC values for the soil samples at Ap horizon, A horizon and UPRM. It indicates that soil sample from UPRM has higher CEC. The CEC for the Ap horizon is large than A horizon probably due to a higher content of organic matter. In order to obtain a good estimate of the CEC and adsorption capacity of the clay fractions the pH for the clay suspension (See tables 5.2) was adjusted from 5.5 to 6.0 by addition of diluted acid or base. The CEC for the clay fraction from A horizon has higher CEC than from Ap horizon and UPRM. The presence of charge on colloidal systems influences its ability to attract or repulse charge ions to or from surfaces. The importance of cation exchange at negative sites is that it is the major retention mechanism for heavy metals and other contaminants such as nitroaromatic and nitroamine compounds.

Table 5.2 Properties of the clay fractions from Ap, A horizons and UPRM used in RDX adsorption studies.

Horizons	pH	Surface Area (m²/g)	CEC (meq/100g)
A	5.5-6.0	414.87	13.12
Ap	5.5-6.0	357.71	12.50
UPRM	5.5-6.0	231.97	11.87

5.3 Surface Area Analysis for Soil and Clay Samples

Surface area is a fundamental property that can be used as identification criterion. This property is dependent of the size of the mineral particles; smaller particles have larger surface area. It gives us an estimate of the available area for cation exchange and adsorption of other species like pesticides and other contaminants. As we can see in table 5.1 the soil sample from UPRM has a greater surface area than Ap horizon and A horizon. If we analyzed the clay fraction (See tables 5.2), it has a greater surface area than the soil samples. This is because clay minerals have smaller particle sizes in comparison with soil which is constituted of sand, silt and clay particles, and organic matter. Also, some clay minerals have external and internal surfaces which are an additional contribution to the total surface area. In contrast to the results found for the soil samples, clay samples from A horizon have more higher surface area than those from Ap horizon and UPRM clay (Tables 5.2). This is indicative of the presence of finer clay fractions and larger percentage of expandable clay in the A horizons.

5.4 X-Ray Diffraction Analysis for the Clay Fraction

X-ray diffraction is a good tool for qualitative mineralogical analysis. A common clay mineral found in all the samples was kaolinite. This clay mineral is characterized by two x-ray diffraction peaks at diffraction angles of 12.2 and 24.7. Kaolinite is abundant in the clay fraction as product of weathering and it is a common constituent in tropical conditions ⁽⁵⁾. It is the clay mineral with larger particle size. The common structure of Kaolinite consists of Al in an octahedral sheet and Si in a tetrahedral sheet. The layers are bound to each other by H bonding between oxygens of the tetrahedral sheet and the hydroxyls of the next octahedral sheet as shown in Figure 5.3. Its specific surface is small in comparison with other clay minerals as illite and montmorillonite. Illite was found in the clay fraction UPRM, this clay mineral is characterized by a series of x-ray diffraction peaks at diffraction angles of 8.8, Illite is a non-expanding clay fraction. Iron oxides, like hematite and goethite, were found in the clay fractions too. Hematite with a molecular formula of Fe_2O_3 is a common iron oxide which exhibits a characteristic peak in the 2 theta scale at 33.3. It is the responsible of the red color in soils. On the other hand, goethite with a molecular structure of FeOOH shows a characteristic peak at 21.3, it is responsible of the yellow color in soils, and it is the most abundant of the iron oxides. These minerals were present in all samples as shown in figures 5.4, 5.5 and 5.6. Another mineral was gibbsite; the main peak for this mineral was around 20.0 degrees 2 theta. Gibbsite is the most common aluminum oxide in soils and in our studies it was found in all the samples analyzed. Quartz was also observed in the x-ray

diffraction analysis. This mineral exhibits characteristic peaks at 20.8 and 27.0 in the 2 theta scale. Quartz is the other major component mineral found in this fraction and probably the only mineral more common in soils than kaolinite because of its extreme durability ⁽¹⁹⁾.

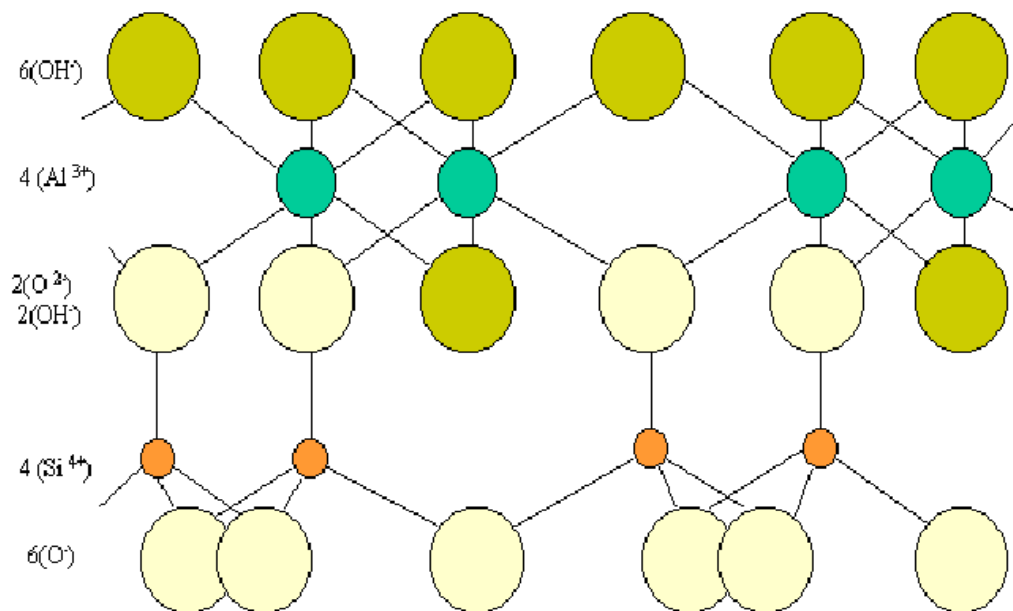


Figure 5.3. Structural diagram for kaolinite showing the hydroxyl and siloxane surfaces.

From: http://www.ucm.es/info/crismine/Edafologia_Mercedes/Minerales_arcilla

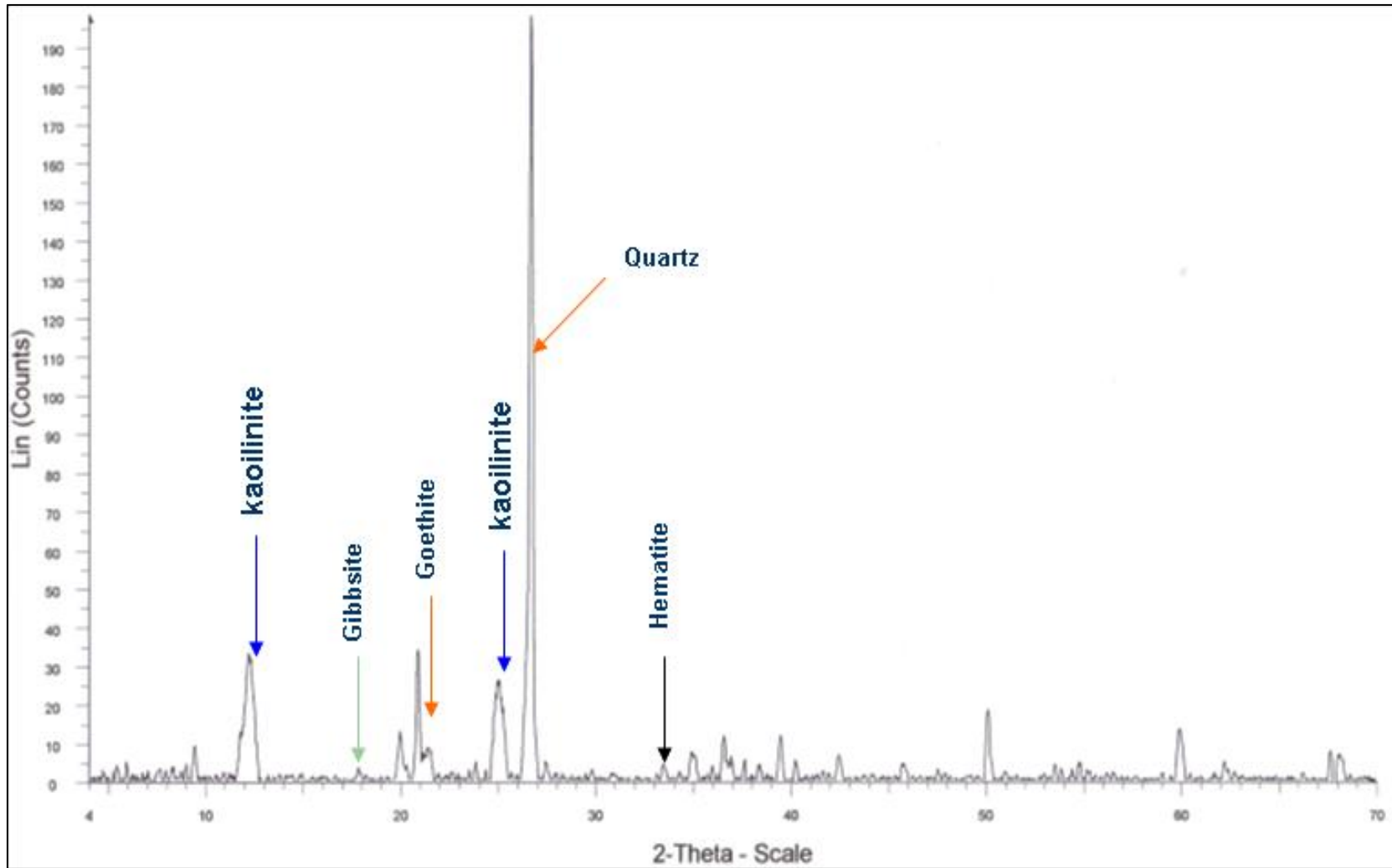


Figure 5.4 X-ray diffraction mineral characterization of the clay fraction from A horizon.

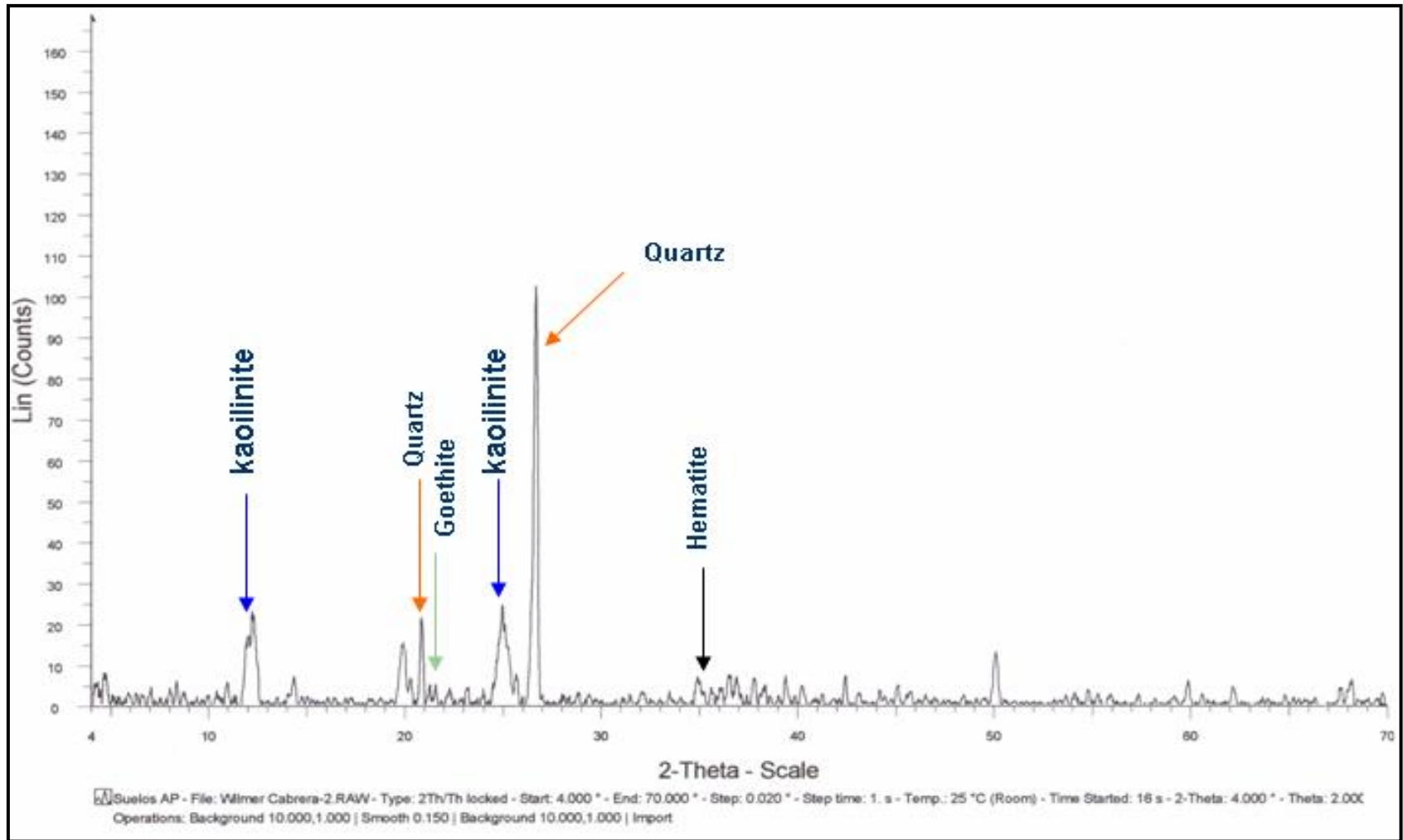


Figure 5.5 X-ray diffraction mineral characterization of the clay fraction from Ap horizon.

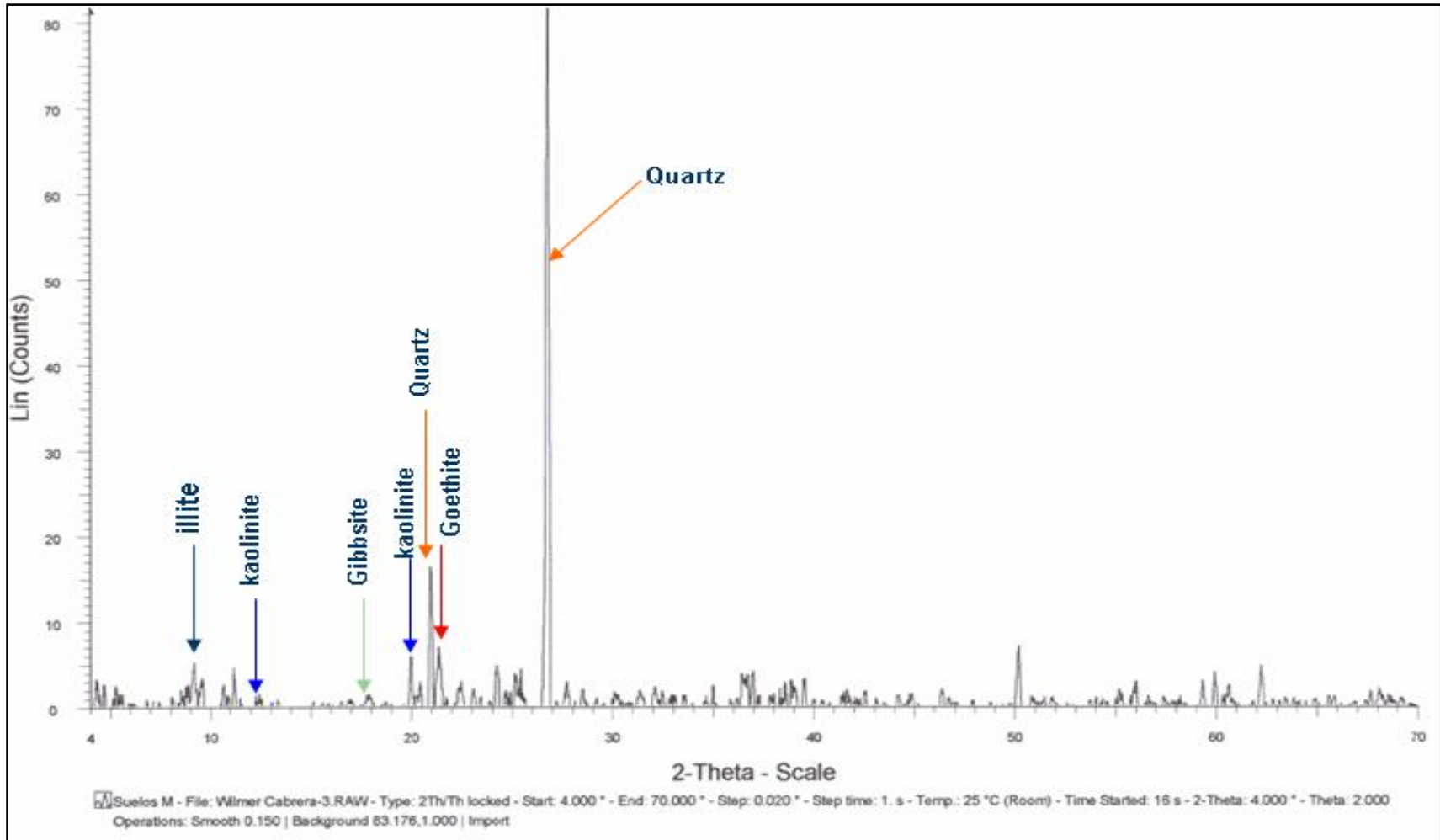


Figure 5.6 X-ray diffraction mineral characterization of the clay fraction from UPRM.

5.5 Methodology Validation for RDX Adsorption Studies

Two peaks appear in the chromatogram showed in figure 5.7. This chromatogram was obtained injecting 5 μL of 12 ppm RDX aqueous solution. The first peak around 1.312 min corresponds to the sample solvent. This was confirmed running a blank solution, which contains only 0.1 M KCl in deionized water. The second peak with retention time of 3.011 min corresponds to RDX, the analyte under study. In order to know if the separation of the analyte occurs in a reasonable period of time, the capacity factor was calculated. This parameter is used to describe the migration rate of the analyte in the chromatographic column. The value obtained for this parameter was 2.0 which is in the accepted range of 1 to 5. The precision of the method was also evaluated. The reproducibility of the method with regard to retention time and peak area was evaluated using the 12 ppm RDX standard solution. Relative standard deviation (% RSD) for retention time was 0.0 % and for peak area it was 0.02 % (See tables 5.4 y 5.5). The values for % RSD are excellent since values lower than 2% for the retention time and for the peak area are generally considered of satisfactory precision.

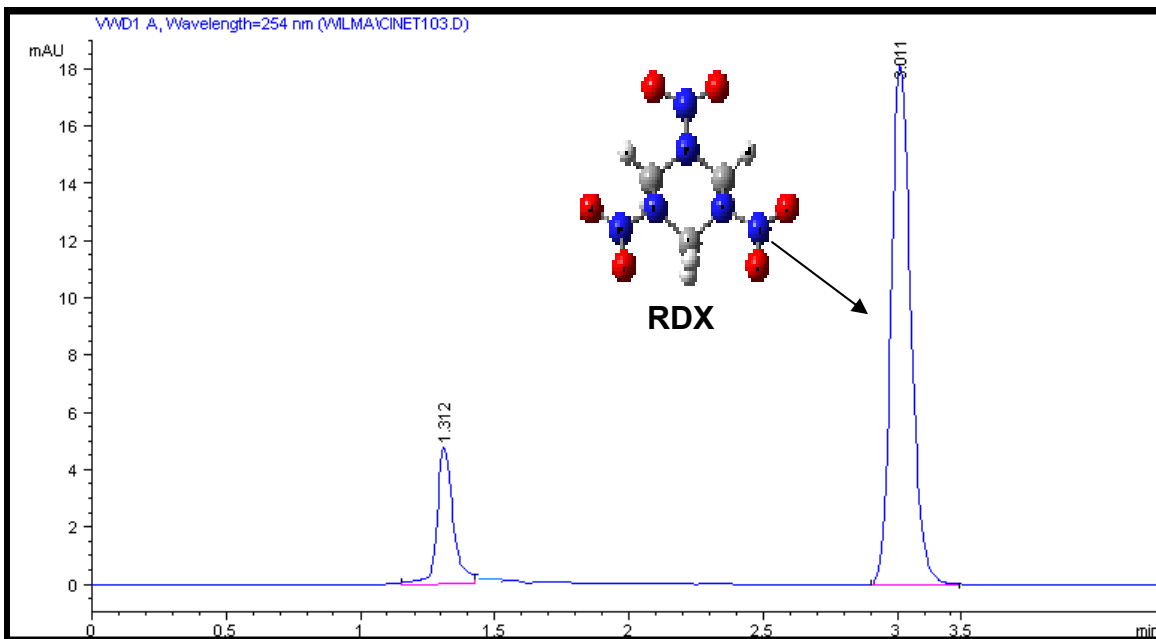


Figure 5.7 Chromatogram for 12 ppm RDX aqueous solution.

In order to evaluate the limit of linearity, a calibration curve was constructed using RDX concentrations in a range of 0 ppm to 40 ppm. A RDX concentration of 24 ppm was the highest concentration maintaining a linear relationship (See figure 5.8). Therefore, the accepted range used for RDX adsorption studies goes from 0 to 24 ppm. The limit of detection (LOD) of the system was 0.610 ppm. It was found a limit of quantification (LOQ) of 2.030 ppm, this concentration can be determined with acceptable precision and accuracy. Other calibration curves used in RDX adsorption studies are presented in Appendix 1.

Table 5.3 Evaluation of the area for RDX peak in aqueous solution at different concentrations: average area, standard deviation, and relative standard deviation.

Concentration (ppm)	Area 1 (mAU)	Area 2 (mAU)	Area 3 (mAU)	Average Area (mAU)	Standard Deviation	Relative Standard Deviation
0.00	0.00	0.00	0.00	0.00	0.00	0.00
4.00	31.435	31.399	31.352	31.395	0.042	0.13
8.00	59.187	59.075	58.579	58.947	0.324	0.55
*12.00	88.129	88.147	88.110	88.129	0.019	0.02
16.00	120.233	120.418	120.267	120.306	0.098	0.08
20.00	149.152	149.258	149.174	149.195	0.056	0.04
24.00	179.988	180.002	180.151	180.047	0.090	0.05

*RDX standard solution used to evaluate reproducibility

Table 5.4 Evaluation of retention time for RDX peak in aqueous solution at different concentrations: average retention time, standard deviation, and relative standard deviation.

Concentration (ppm)	Retention Time 1 (min)	Retention Time 2 (min)	Retention Time 3 (min)	Average Retention Time (min)	Standard Deviation	Relative Standard Deviation
0.00	0.000	0.000	0.000	0.000	0.000	0.000
4.00	3.038	3.038	3.036	3.037	0.001	0.038
8.00	3.035	3.034	3.034	3.034	0.001	0.019
*12.00	3.011	3.011	3.011	3.011	0.000	0.000
16.00	3.039	3.039	3.039	3.039	0.000	0.000
20.00	3.035	3.025	3.034	3.031	0.006	0.182
24.00	3.039	3.037	3.035	3.037	0.002	0.066

*RDX standard solution used to evaluate reproducibility

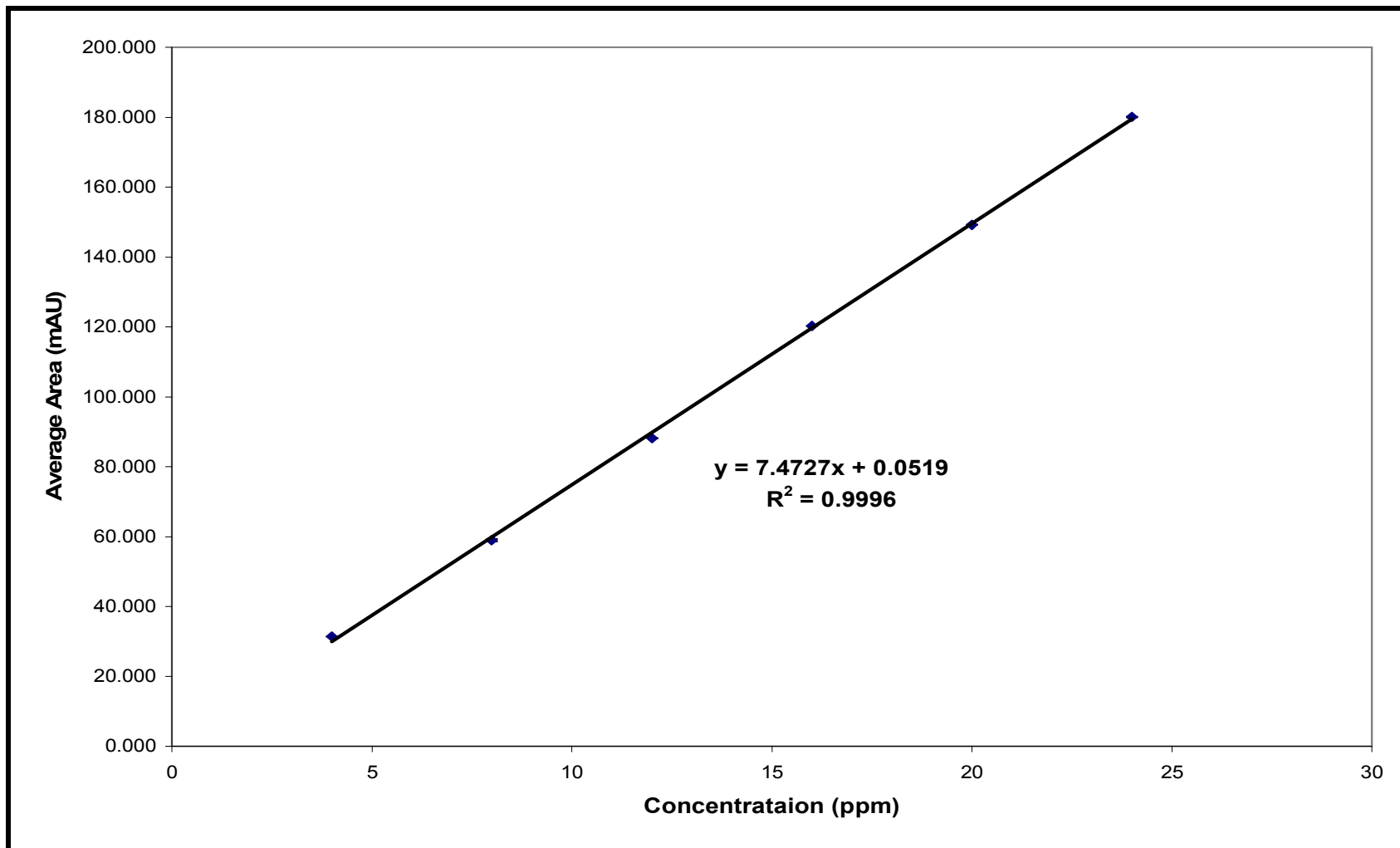


Figure 5.8 Calibration curve for RDX in aqueous solution: Average Area vs. Concentration

5.6 Sorption Kinetics

The RDX adsorption by Jobos soil series and clay mineral as a function of time is presented in figure 5.9. The rates of adsorption for RDX in soil and clay were similar. Equilibrium between the adsorbed and aqueous phases was achieved within 5-7 hours. Although the equilibrium was achieved between 5-7 hours, the studies of adsorption were conducted with an equilibrium time of 22 hours to look for potential products of degradation of RDX. However, no degradation products of RDX were observed.

5.7 Adsorption Isotherms

RDX adsorption on soil samples was modeled very well by the Freundlich isotherm, as can be seen, in figure 5.10. The linear expressions of the Langmuir and Freundlich equations (See equations 3.5 and 3.7) were used to determine experimental adsorption coefficients (the inverse of the slope) and retention energies (the inverse of the intercept) (See figures 5.11 and 5.12). The experimental adsorption coefficients for RDX-soil interactions are summarized in table 5.6. Values for the correlation factor (r^2) near one were found in the linear representation of the Freundlich model for the soils samples. It was observed an adsorption coefficient (K_d) of 0.998 L/Kg for UPRM soil, 0.653L/Kg for Ap horizon and 0.458 L/Kg for A horizon. The low K_d value for RDX sorption is in agreement with literature values (0.97 L/Kg⁽⁷⁾, 0.21-0.33 L/Kg⁽²⁰⁾, 0.3-0.7 L/Kg⁽²¹⁾). These values indicate limited affinity of RDX for soil surfaces and high potential for

transport. UPRM soil shows a greater adsorption coefficient than AP horizon and A horizon. The greater adsorption coefficient of UPRM soil can be attributed to its high percent the clay (53.7%) in the soil sample and greater cation exchange capacity (6.75 cmol/Kg). The greater adsorption coefficient of Ap than A horizon can be attributed to its high organic matter content (6 %) ⁽²²⁾.

The nature of soil organic matter (SOM) is highly colloidal. Soil organic matter, also known as humic material, is composed as humic substances which are the most chemically active compounds in soils. They have electrical charges and exchange capacities that exceed those of the clay minerals. The chemical behavior of humic matter is in general controlled by the carboxyl and phenolic-OH functional groups. These functional groups present pH-dependent charges; they dissociate their protons making the humic molecule negative charged. Due to the presence of these charges and the great heterogeneity of soil organic matter a number of reactions can take place. Hydrogen bonding, ion-dipole interaction or coordination, ionic bonding, water bridging, and van der Waals bonding forces can take place between humic matter and clay minerals ⁽¹⁹⁾. Also, soil humic material is in general hydrophobic which can cause the accumulation of hydrophobic pollutants in the soil matrix ^(23, 24). The variety of binding mechanisms mentioned above also should be applicable to synthetic organics introduced to soil, such as herbicides, pesticides, and industrial waste organic compounds.

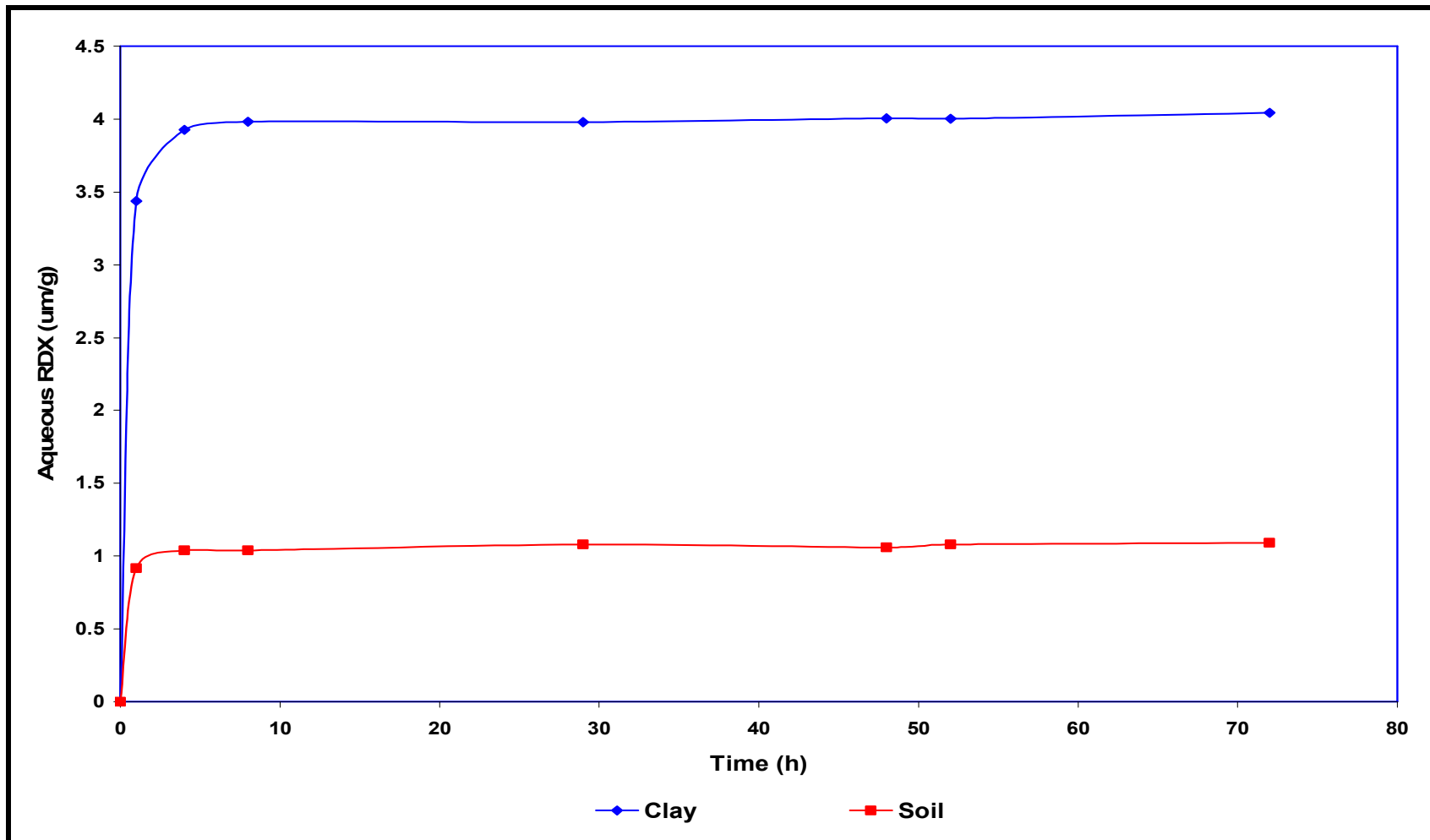


Figure 5.9 Kinetics of adsorption of RDX on soil and clay Ap horizon.

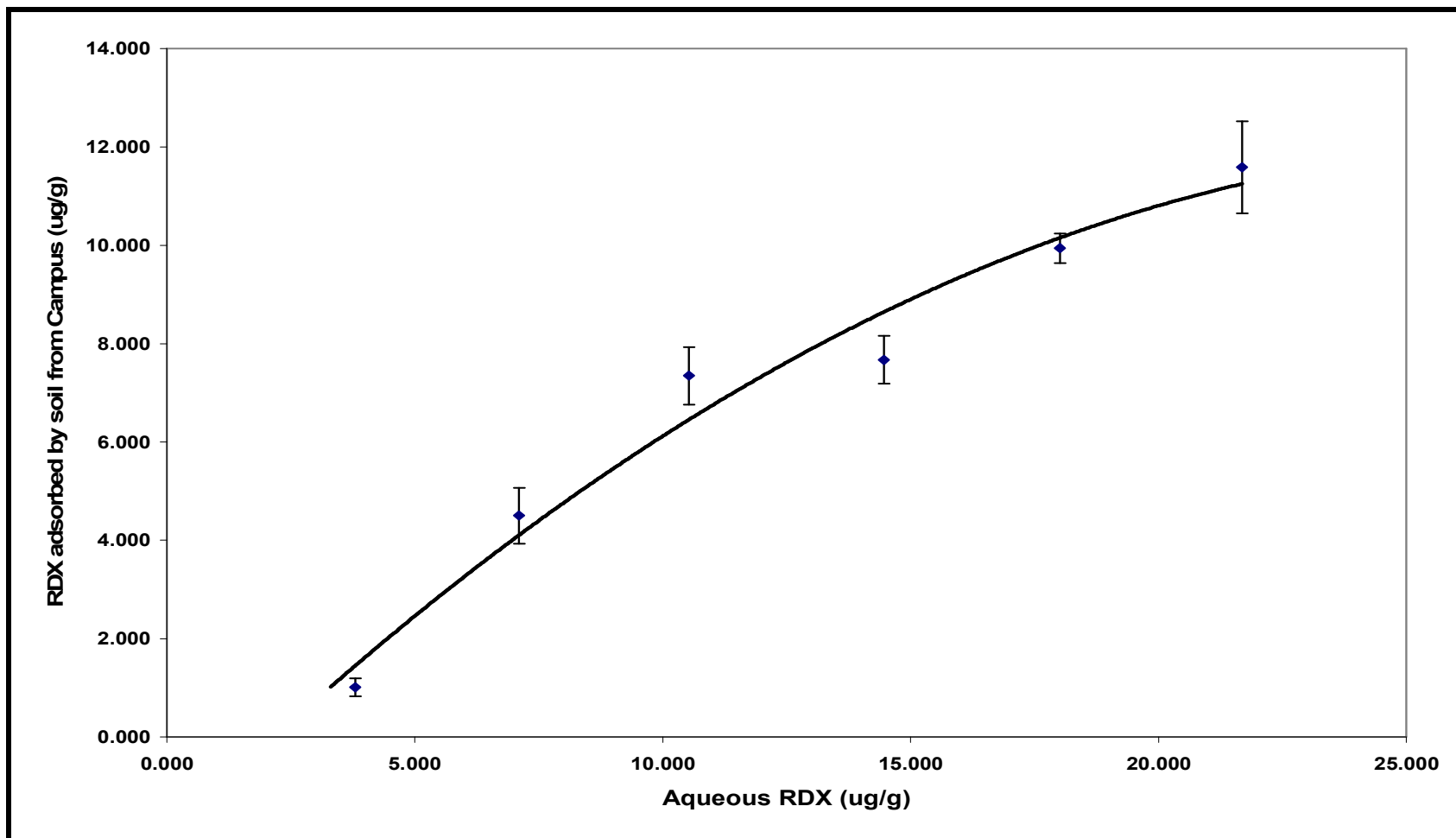


Figure 5.10 Adsorption isotherm for RDX on soil from UPRM.

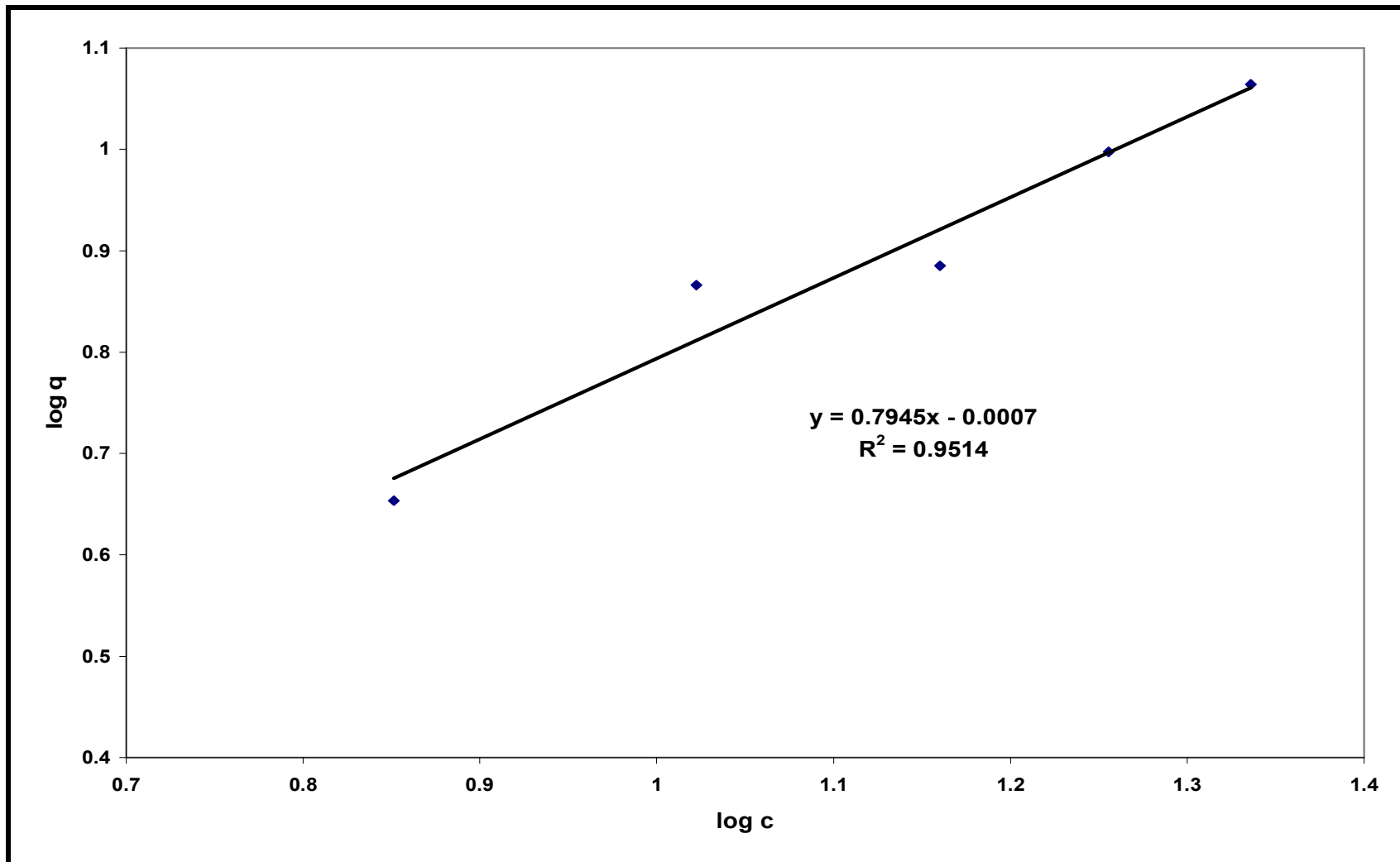


Figure 5.11 Freundlich linear representation for RDX adsorption on soil from UPRM.

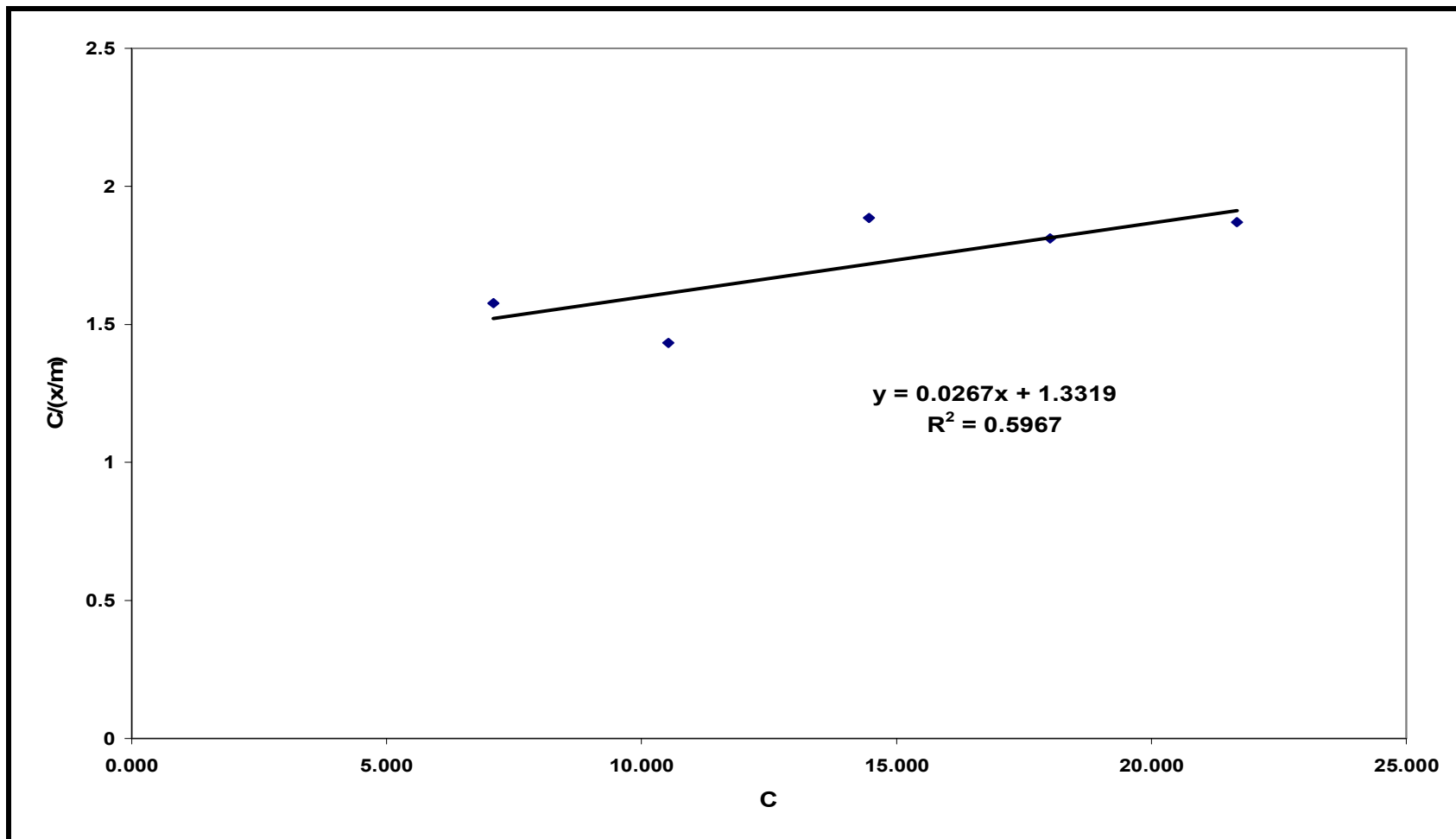


Figure 5.12 Langmuir linear representation for RDX adsorption on soil from UPRM.

Figure 5.13 shows representative example of the type of adsorption isotherms obtained for RDX in aqueous suspensions of homoionic K^+ -clay minerals. The shape of this isotherm can be approximated to the Freundlich equation 3.4. The Freundlich isotherm model was selected for the clay samples because a better linear representation was observed (See figures 5.14 and 5.15). This assumption was done taking into consideration that clay minerals are a reactive system in which more adsorption could take place.

The linear representation of the Freundlich equation gives a relative adsorption capacity (the antilog of the intercept), increase in the order UPRM clay (3.76 L/Kg) < Ap horizon (3.99 L/Kg) < A horizon (4.42 L/Kg). The clay fraction from UPRM presents a smaller adsorption capacity in comparison with clay fraction from the A horizon and AP horizon. The sorption capacity constant for RDX in clay minerals is considerably low and these values indicate limited affinity of RDX for clay minerals and a high potential for transport. Another characteristic associated with the adsorption of RDX by the clay fraction is the affinity (the slope) of the clay for this nitroamine compound. The A horizon demonstrates a major affinity than the Ap horizon and UPRM clay. The clay from A horizon showed a largest surface area (414.87 m^2/g), which may have contributed to the higher adsorption of RDX.

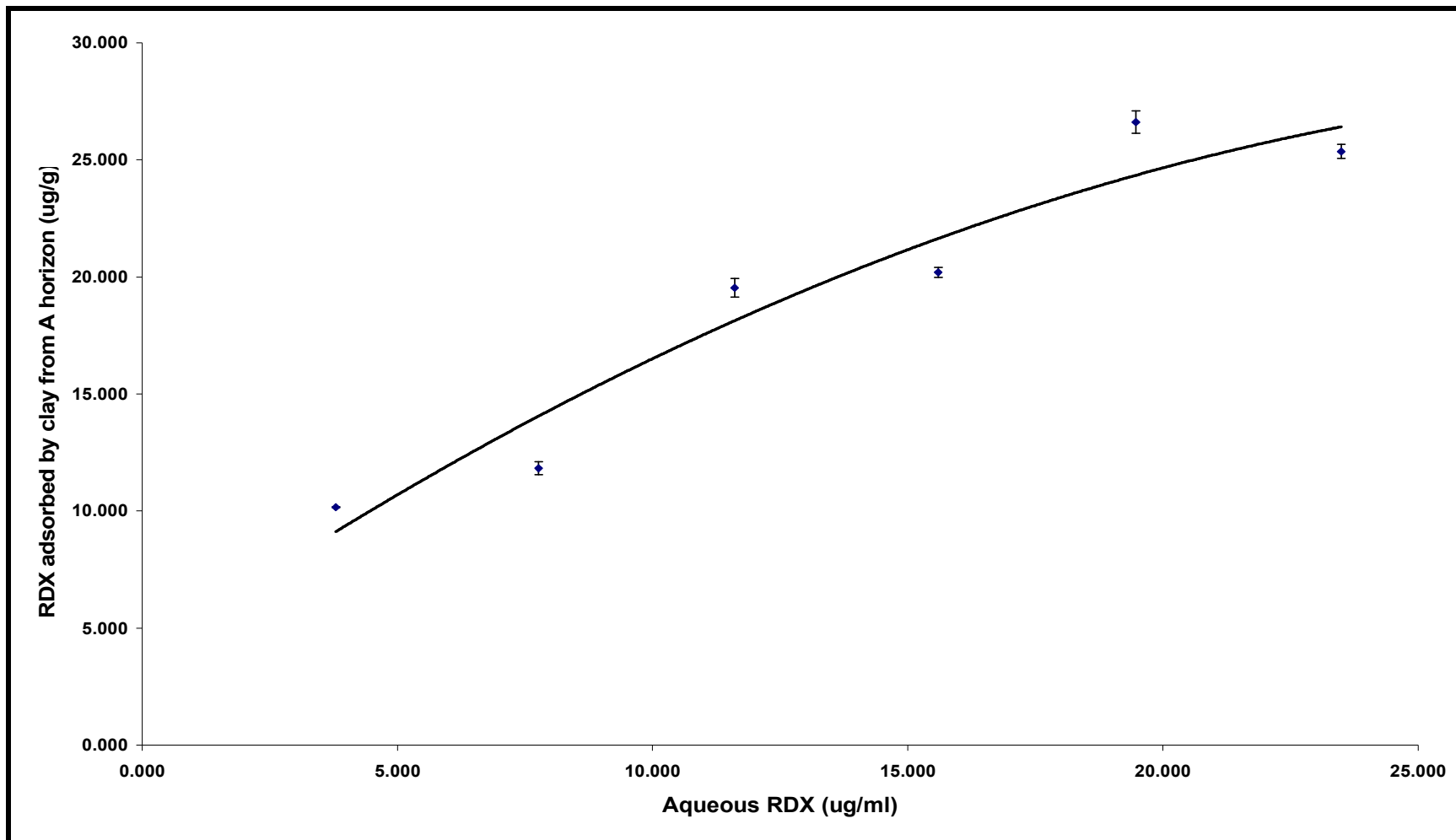


Figure 5.13 Adsorption isotherm for RDX on clay fraction from A horizon.

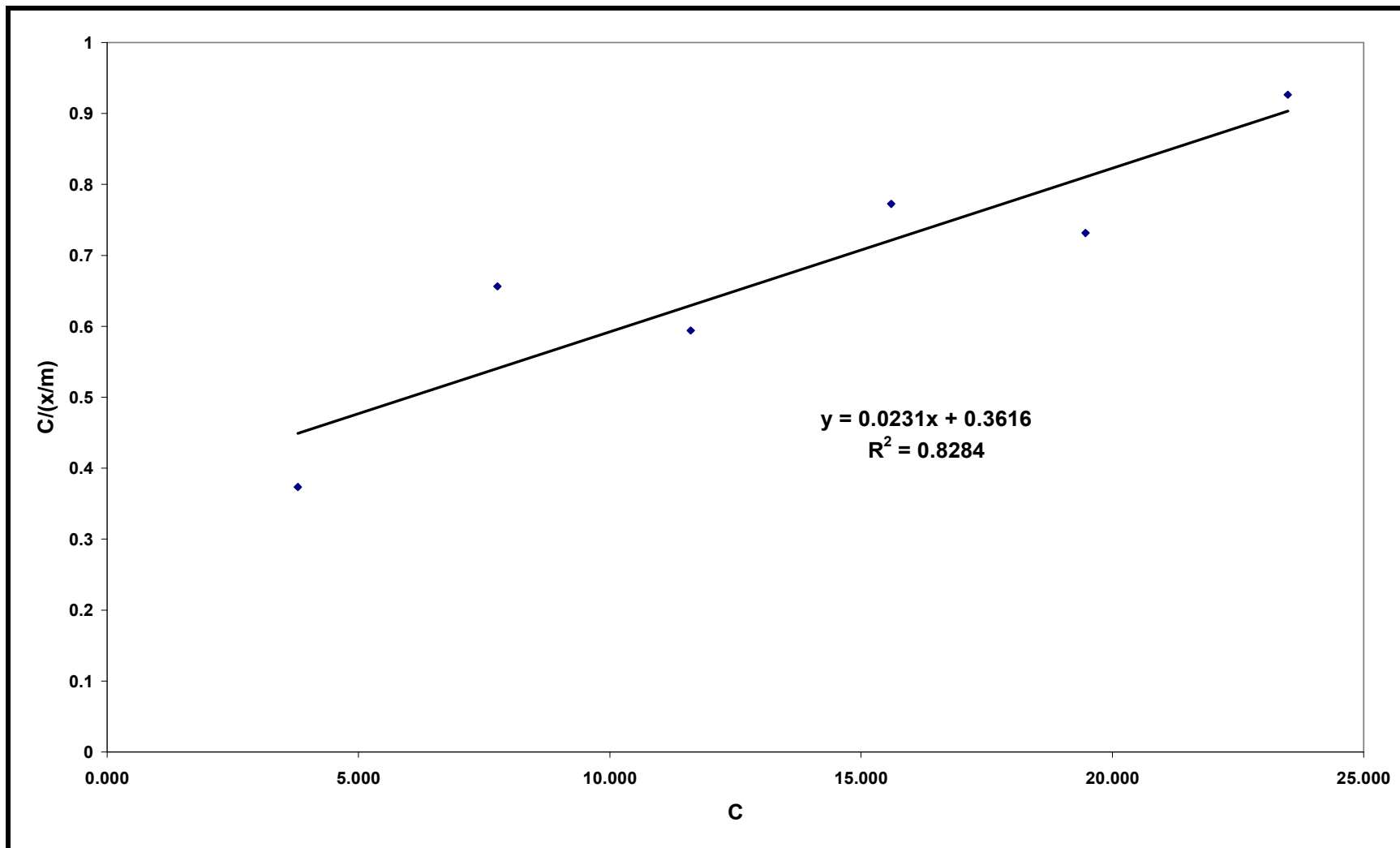


Figure 5.14 Langmuir linear representation for RDX adsorption on clay fraction from A horizon.

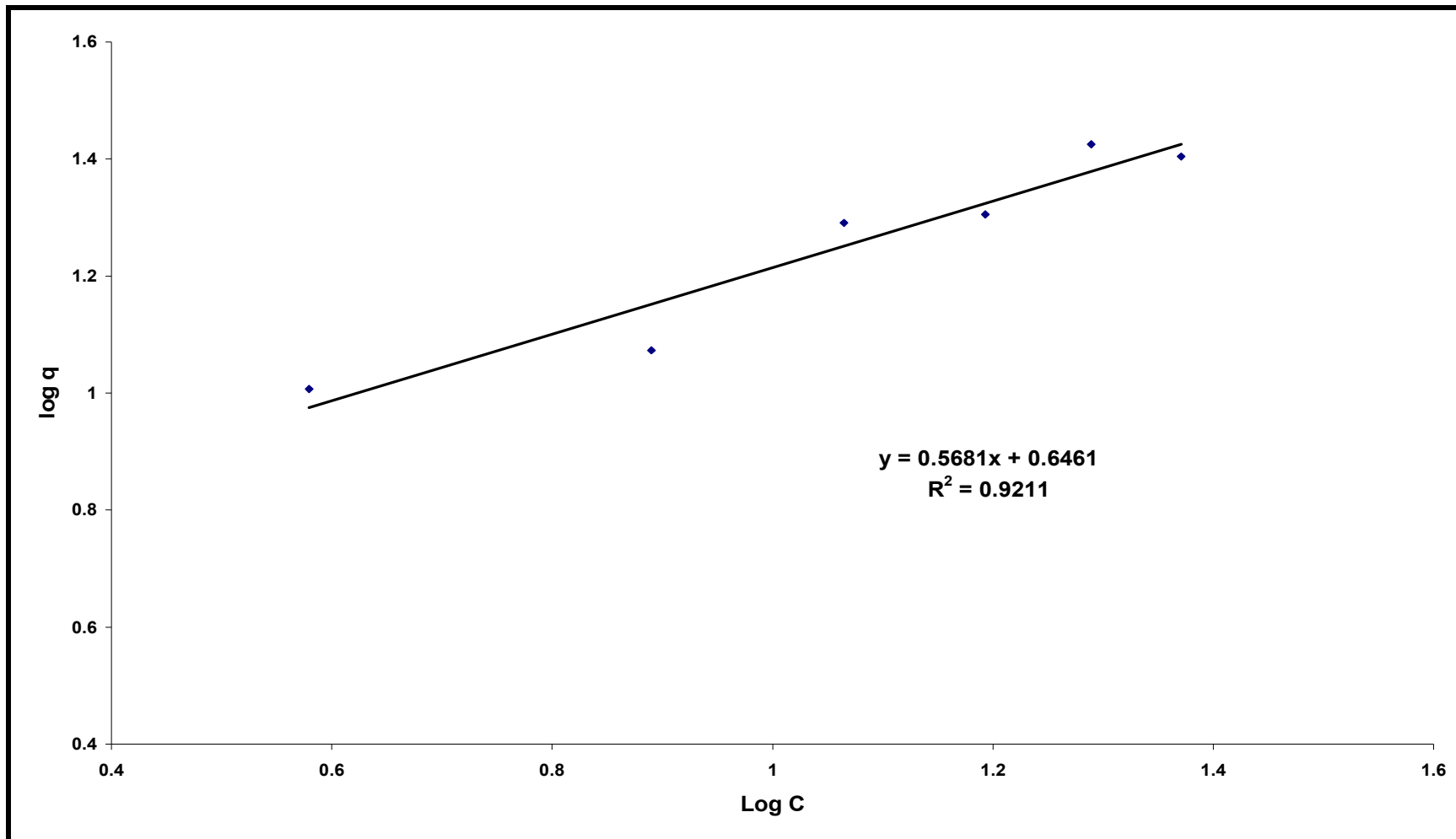


Figure 5.14 Freundlich linear representation for RDX adsorption on clay fraction from A horizon.

Table 5.5 Summary of regression parameters for RDX adsorption on soil and clay from Ap, A horizons and UPRM.

Sample ID	Freundlich Isotherm			Langmuir Isotherm		
	Relative Adsorption (L/Kg) (K_d)	Affinity (n)	r^2	Maximum Adsorption (mg/Kg) (b)	Retention Constant (K)	r^2
A-Soil	0.46	1.259	0.9514	37.45	0.7508	0.5970
Ap-Soil	0.65	0.995	0.9504	38.76	1.032	0.8128
UPRM-soil	0.99	1.250	0.8001	37.45	0.356	0.0750
A-clay	4.42	1.760	0.9211	43.29	2.765	0.8284
Ap-clay	3.99	1.826	0.9464	36.76	2.395	0.8471
UPRM-clay	3.76	2.084	0.8984	25.00	2.199	0.8962

Experimental Adsorption Enthalpy

The adsorption coefficient (K_d) for different isotherms were determined by modeling the data from the Freundlich equation. The adsorption enthalpy was determined using the Van't Hoff equation:

$$\left(\frac{\partial \ln K}{\partial T} \right)_{\ominus} = \frac{\Delta H_{ADS}^{\circ}}{RT^2}$$

The linear representation of the Van't Hoff equation is:

$$\ln K_d = \frac{\Delta S_{ads}}{R} - \frac{\Delta H_{ads}}{R} \frac{1}{T}$$

Therefore, a plot of the natural logarithm of the adsorption coefficient versus the reciprocal temperature gives a straight line. The slope of the line is equal to minus the standard enthalpy change divided by the gas constant, $\Delta H^{\circ}/R$, and the intercept define the value of ΔS_{ads} ($-60.63 \text{ J mol}^{-1} \text{ K}^{-1}$) (see figure 5.15). The experimental adsorption enthalpy (ΔH_{ads}) found for RDX and soil surface interactions was $\Delta H_{ads} = -18.46 \text{ KJ/mol}$. This value is typical of a physical adsorption and suggests that the RDX-soil interactions are of the Van der Waals type. Experimental studies have demonstrated that explosives may adsorb specifically and reversibly to the siloxane surface of the clay mineral kaolinite, which is one of the clay minerals present in the clay fractions studied. Also, the IR and FTIR studies indicate that the vibrational modes presenting

changes correspond to the C-N, N-N bonds and the NO₂ groups suggesting that the electron donor nitrogen atoms from RDX are interacting with the electron acceptor oxygen atoms of the edge sites of the clay's surface⁽²⁵⁾.

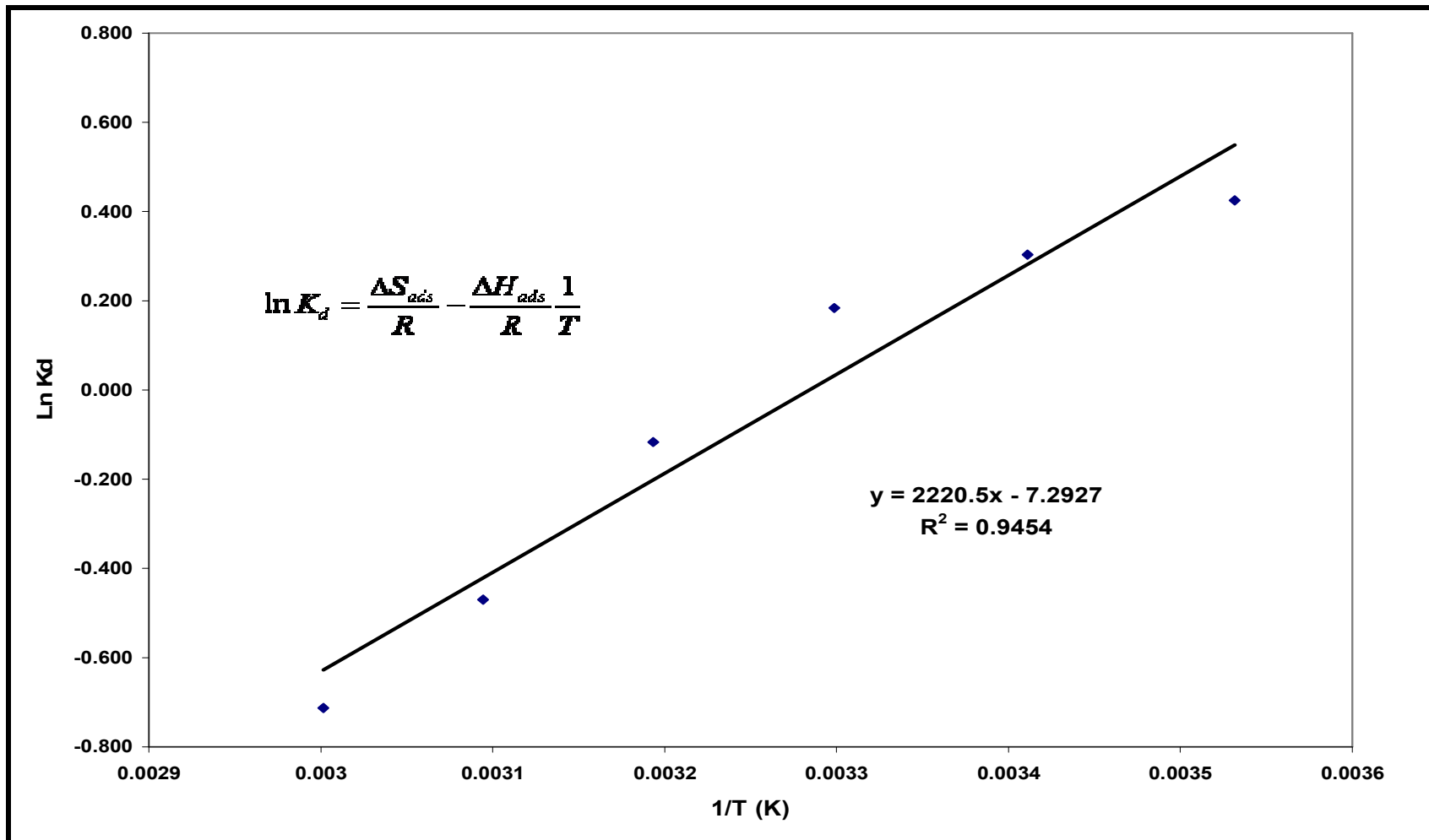


Figure 5.15. Temperature dependence of Kd of RDX: Sorben, Ap horizon soil.

6. CONCLUSIONS

X-ray analysis revealed the presence of kaolinite, goethite, hematite, gibbsite, and quartz as clay minerals. The Kaolinite was the only phyllosilicate found in the clay fractions. Adsorption coefficients for RDX were obtained using High Performance Liquid Chromatography (HPLC). The rates of adsorption for soil and clay were similar. In general, an equilibrium between the adsorbed and aqueous phase of each explosive was achieved within 5-7 h. After 22 h of adsorption process on soil and clay mineral, degradation products of RDX were not detected.

The Freundlich model described the adsorption process in soil and clay mineral samples. Adsorption studies performed in soil samples demonstrated a high adsorption coefficient in the UPRM soil. The greater adsorption coefficient of UPRM soil can be attributed to its high percent the clay (53.7%) in the soil sample and greater cation exchange capacity (6.75 meq/100g). The Ap horizon which contains more organic matter has a greater adsorption coefficients than A horizon. In contrast to soil samples, when the adsorption studies were performed in the clay fractions a tendency to adsorb more in the A horizon was observed. These observations allow us to conclude that organic matter contributes significantly to the adsorption process in soil samples. On the other hand, properties like cation exchange capacity, surface area, type of exchangeable cations and clay mineral present in the samples are important factors in the adsorption of clayey soils.

The low K_d value indicates limited affinity of RDX for soil surfaces and high potential for transport. The experimental adsorption enthalpy ($\Delta H_{ads} = -18.46$ KJ/mol) found for RDX and soil surface interactions, is a value typical of a physical adsorption and suggests that the RDX-soil interactions are of the Van der Waals type. This work provides a better understanding of the behavior of RDX in soil environment in order to establish optimum conditions for its detection, fate, and transport process.

7. RECOMMENDATIONS

For a better understanding of the interactions between chemical explosives and soil environment, it is recommended to:

- Monitor the long-term fate of RDX during a period of time in the aqueous and solid phases.
- To identify and quantify the degradation products from RDX in soil and mineral surface.
- Perform RDX adsorption studies with different phyllosilicate (illite, kaolinite and montmorillonite).
- To study microbial degradation of RDX.

8. REFERENCES

1. Sheremata, T.W.; Halasz, A.; Paquet, L.; Thiboutot, S.; Ampleman, G.; Hawari, J. The fate of the cyclic nitramine explosive RDX in natural soil. *Environ. Sci. Technol.* **2001**, *35*, 1037-1040.
2. Byung-Taek Oh and Alvarez, P, J. Hexahydro-1,3,5-Trinitro-1,3,5-Triazine (RDX) Degradation in Biologically-active iron Columns. *Water, Air, and Soil Pollution* 141: 325–335, **2002**.
3. Haderline, S. B.; Weissmahr, K. W.; Schwarzenbach, R. P. Specific Adsorption of Nitroaromatic Explosives and Pesticides to Clay Minerals, *Environ. Sci. Technol.* **1996**, *30*, 612-622
4. Brady, N.C.; and Weil, R.R. The Nature and Properties of Soils, Prentice Hall, New Jersey, **2002**.
5. Schulze, D. G. Soil Mineralogy with Environmental Applications, SSSA Book Series No. 7, Chapter 1, *Soil Science of America*, Inc., Madison, Wisconsin, **2002**.
6. Haderlein, S. B.; and Schwarzenbach, R. P. Adsorption of substituted nitrobenzenes and nitrophenols to mineral surfaces, *Environ.Sci.Technol.* **1993**, *27*, 316-326.
7. Singh, J.; Confort, S.D.; Hundal, L.S. and Shea, P.J. Long-Term RDX sorption and fate in soil. *Environ.Qual.***1998**, *27*,572-577.
8. Deborah R. Felt, Steven L. Larson, Altaf Wani, and Jeffrey L. Davis. Analysis of RDX and RDX breakdown products in environmental samples. Environmental Laboratory, US Army Engineer Research and Development Center, Vicksburg. **2003**, MS 39180-6199.
9. McCormick, N. G., Cornell, J. H., and Kaplan, A. M. Biodegradation of Hexahydro-1,3,5-Trinitro-1,3,5-Triazine. *Appl. Environ. Microbiol.* **1981**,*42*, 817.
- 10.Hatzinger, Paul B., Fuller, Mark E., Rungmakol, Darin, Schuster, Rachel L., Steffan, Robert. Enhancing the attenuation of explosives in surface soils at military facilities: Sorption–Desorption isotherms. *Environmental Toxicology and Chemistry.* **2004**, *23*, 306-312.
- 11.Davis, T. The chemistry of powder and explosives. GSG Publishers. 141pp. **1998**.

12. Yinon, J. Forensic and Environmental Detection of Explosives, John Wiley and Sons, Ltd., NY, **1999**.
13. Skoog, D.A.; West, D.M.; Holler, F.J. Fundamentals of Analytical Chemistry 7th Edition, Saunders College Publishing, Philadelphia, **1996**.
14. Skoog, D. A.; Holler, F. J.; Nieman, T. A. Principles of Instrumental Analysis 5th Edition, Thomson Learning, Inc., United States, **1997**.
15. Yinon, J.; Zitrin, S. Modern Methods and Applications in Analysis of Explosives, John Wiley and Sons, Ltd., NY, **1993**.
16. Klute A., Campbell G. S., Jackson R. D., Mortland M. M., Nielsen D. R., Methods of Soil Analysis Part 1: Physical and Mineralogical Methods, 1118, American Society of Agronomy, Inc., Madison Wisconsin. **1986**
17. EPA Method 8330. Nitroaromatics and Nitramines by High Performance Liquid Chromatography. U.S. Environmental Protection Agency. Office of Soil Waste and Emergency Response, Washington, D.C., SW-846 Revision 0, **1994**.
18. R.B. Brown, professor emeritus, Soil and Water Science Department, Florida Cooperative Extension Service, Institute of Food and Agricultural Sciences, University of Florida, Gainesville, FL 32611-0510, **2003**.
19. Monger, H.C.; Kelly, E.F. Soil Mineralogy with Environmental Applications, SSSA Book Series No. 7, Chapter 3, *Soil Science of America*, Inc., Madison, Wisconsin, **2002**
20. Pennington, J. C.; Bowen, R.; Brannon, J. M.; Zakikhani, M.; Harrelson, D. W.; Gunnison, D.; Mahannah, J.; Clarke, J.; Jenkins, T. F.; Gnewuch, S. Draft Protocol for Evaluating, Selecting, and Implementing Monitored Natural Attenuation at Explosives-Contaminated Sites; Technical Report EL-99-10; U.S.ArmyCorps of Engineers, Engineer Research and Development Center: Vicksburg, MS, **1999**.
21. Monteil, F, R; Groon, C; Hawari, A. Sorption and Degradation of Octahydro 1,3,5,7-tetranitro-1,3,5,7-tetrazocine in Soil. *Environ. Sci. Technol.***2003**, 37, 3878-3884.
22. Rivera, R.V, TNT Adsorption on Jobos soil and Jobos clay fraction . M.S. Thesis, University of Puerto Rico, Mayagüez, PR, **2006**.
23. Koopal, L. K.; van Reimsdijk, W. H.; Kinniburgh, D. G. Humic Matter and Contaminants. General Aspects and Modeling Metal Ion Binding. *Pure Appl. Chem.* **2001**, 73, 2005-2016.

24. Semple, K.T.; Morriss A.W.J.; Paton, G.I. Bioavailability of Hydrophobic Contaminants in Soils: Fundamental Concepts and Techniques for Analysis, *Eur. J. Soil. Sci.* **2003**, *54*, 809-818.
25. Colón, Y.M.; Alzate, L.F.; Ramos, C.M.; Santana, A.; Hernández, S.P.; Castro, M.E.; Muñoz, M.A.; Mina, N. "Adsorption of RDX on Clay," in *Proceedings of SPIE Vol. 5415, Detection and Remediation Technologies for Mines and Minelike Targets VIII*, edited by Russell S. Harmon, John H. Holloway, Jr., J.T. Broach, (SPIE, Bellingham, WA, **2004**) 1419-1430.

APPENDIX A

Adsorption Models and Linear Representation

Table A.1 Experimental results for RDX interaction with soil from UPRM.

Sample ID	RDX Initial Concentration (ppm)	Area 1 (mAU)	Area 2 (mAU)	Average Area (mAU)	Concentration at equilibrium (ug/mL)	Mass in aqueous solution (ug)	Adsorbed mass (ug)	RDX adsorbed by topsoil (mg/kg)
1a	4.00	29.113	27.996	28.555	3.786	37.865	2.135	1.068
2a	8.00	52.222	52.394	52.308	6.976	69.762	10.238	5.119
3a	12.00	79.069	79.155	79.112	10.575	105.755	14.245	7.123
4a	16.00	108.208	108.455	108.332	14.499	144.992	15.008	7.504
5a	20.00	134.870	134.827	134.849	18.060	180.599	19.401	9.700
6a	24.00	160.660	159.782	160.221	21.467	214.670	25.330	12.665
Sample ID	RDX Initial Concentration (ppm)	Area 1 (mAU)	Area 2 (mAU)	Average Area (mAU)	Concentration at equilibrium (ug/mL)	Mass in aqueous solution (ug)	Adsorbed mass (ug)	RDX adsorbed by topsoil (mg/kg)
1b	4.00	28.472	28.378	28.425	3.769	37.691	2.309	1.155
2b	8.00	53.416	53.393	53.405	7.123	71.234	8.766	4.383
3b	12.00	77.895	77.691	77.793	10.398	103.984	16.016	8.008
4b	16.00	106.804	107.716	107.260	14.355	143.553	16.447	8.224
5b	20.00	134.644	134.624	134.634	18.031	180.311	19.689	9.844
6b	24.00	162.395	162.649	162.522	21.776	217.760	22.240	11.120
Sample ID	RDX Initial Concentration (ppm)	Area 1 (mAU)	Area 2 (mAU)	Average Area (mAU)	Concentration at equilibrium (ug/mL)	Mass in aqueous solution (ug)	Adsorbed mass (ug)	RDX adsorbed by topsoil (mg/kg)
1c	4.00	28.998	28.896	28.947	3.839	38.392	1.608	0.804
2c	8.00	54.042	53.903	53.973	7.200	71.997	8.003	4.002
3c	12.00	79.535	79.323	79.429	10.618	106.180	13.820	6.910
4c	16.00	108.391	108.899	108.645	14.541	145.413	14.587	7.294
5c	20.00	134.316	133.663	133.990	17.945	179.446	20.554	10.277
6c	24.00	162.395	163.047	162.721	21.803	218.027	21.973	10.986

Table A.2 RDX concentrations at equilibrium for three replicates, average concentration, and standard deviation for RDX interactions with soil from UPRM.

Concentration at equilibrium (ug/mL)	Concentration at equilibrium (ug/mL)	Concentration at equilibrium (ug/mL)	Average concentration at equilibrium (ug/mL)	Standard Deviation
3.786	3.769	3.839	3.798	0.037
6.976	7.123	7.200	7.100	0.114
10.575	10.398	10.618	10.531	0.117
14.499	14.355	14.541	14.465	0.098
18.060	18.031	17.945	18.012	0.060
21.467	21.776	21.803	21.682	0.187

Table A.3 Adsorption of RDX by soil for three replicates, average adsorption, and standard deviation for RDX interactions with soil from UPRM.

RDX adsorbed by topsoil (mg/kg)	RDX adsorbed by topsoil (mg/kg)	RDX adsorbed by topsoil (mg/kg)	Average RDX adsorbed by topsoil (mg/kg)	Standard Deviation
1.068	1.155	0.804	1.009	0.183
5.119	4.383	4.002	4.501	0.568
7.123	8.008	6.910	7.347	0.582
7.504	8.224	7.294	7.674	0.488
9.700	9.844	10.277	9.940	0.300
12.665	11.120	10.986	11.590	0.933

Table A.4 Experimental results for RDX interaction with soil from Ap horizon.

Sample ID	RDX Initial Concentration (ppm)	Area 1 (mAU)	Area 2 (mAU)	Average Area (mAU)	Concentration at equilibrium (ug/mL)	Mass in aqueous solution (ug)	Adsorbed mass (ug)	RDX adsorbed by topsoil (mg/kg)
1a	4.00	27.018	27.157	27.088	3.589	35.895	4.105	2.053
2a	8.00	51.106	51.054	51.080	6.811	68.113	11.887	5.944
3a	12.00	76.496	76.743	76.620	10.241	102.408	17.592	8.796
4a	16.00	104.185	104.400	104.293	13.957	139.568	20.432	10.216
5a	20.00	130.270	130.773	130.522	17.479	174.789	25.211	12.605
6a	24.00	157.277	157.029	157.153	21.055	210.551	29.449	14.725
Sample ID	RDX Initial Concentration (ppm)	Area 1 (mAU)	Area 2 (mAU)	Average Area (mAU)	Concentration at equilibrium (ug/mL)	Mass in aqueous solution (ug)	Adsorbed mass (ug)	RDX adsorbed by topsoil (mg/kg)
1b	4.00	26.972	26.928	26.950	3.571	35.710	4.290	2.145
2b	8.00	51.195	51.281	51.238	6.832	68.325	11.675	5.838
3b	12.00	76.07	76.366	76.218	10.187	101.869	18.131	9.066
4b	16.00	105.056	104.460	104.758	14.019	140.193	19.807	9.904
5b	20.00	131.863	132.284	132.074	17.687	176.873	23.127	11.563
6b	24.00	157.691	157.961	157.826	21.145	211.454	28.546	14.273
Sample ID	RDX Initial Concentration (ppm)	Area 1 (mAU)	Area 2 (mAU)	Average Area (mAU)	Concentration at equilibrium (ug/mL)	Mass in aqueous solution (ug)	Adsorbed mass (ug)	RDX adsorbed by topsoil (mg/kg)
1c	4.00	27.276	27.141	27.209	3.606	36.057	3.943	1.971
2c	8.00	50.976	50.997	50.987	6.799	67.987	12.013	6.007
3c	12.00	76.585	76.997	76.791	10.264	102.638	17.362	8.681
4c	16.00	105.591	106.417	106.004	14.187	141.866	18.134	9.067
5c	20.00	129.373	129.926	129.650	17.362	173.618	26.382	13.191
6c	24.00	158.572	158.661	158.617	21.252	212.516	27.484	13.742

Table A.5 RDX concentrations at equilibrium for three replicates, average concentration, and standard deviation for RDX interactions with soil from Ap horizon.

Concentration at equilibrium (ug/mL)	Concentration at equilibrium (ug/mL)	Concentration at equilibrium (ug/mL)	Average Concentration at equilibrium (ug/mL)	Standard Deviation
3.589	3.571	3.606	3.589	0.018
6.811	6.832	6.799	6.814	0.017
10.241	10.187	10.264	10.230	0.040
13.957	14.019	14.187	14.054	0.119
17.479	17.687	17.362	17.509	0.165
21.055	21.145	21.252	21.151	0.099

Table A.6 Adsorption of RDX by soil for three replicates, average adsorption, and standard deviation for RDX interactions with soil from Ap horizon.

RDX adsorbed by topsoil (mg/kg)	RDX adsorbed by topsoil (mg/kg)	RDX adsorbed by topsoil (mg/kg)	Average RDX adsorbed by topsoil (mg/kg)	Standard Deviation
2.053	2.145	1.971	2.056	0.087
5.944	5.838	6.007	5.930	0.085
8.796	9.066	8.681	8.848	0.198
10.216	9.904	9.067	9.729	0.594
12.605	11.563	13.191	12.453	0.825
14.725	14.273	13.742	14.247	0.492

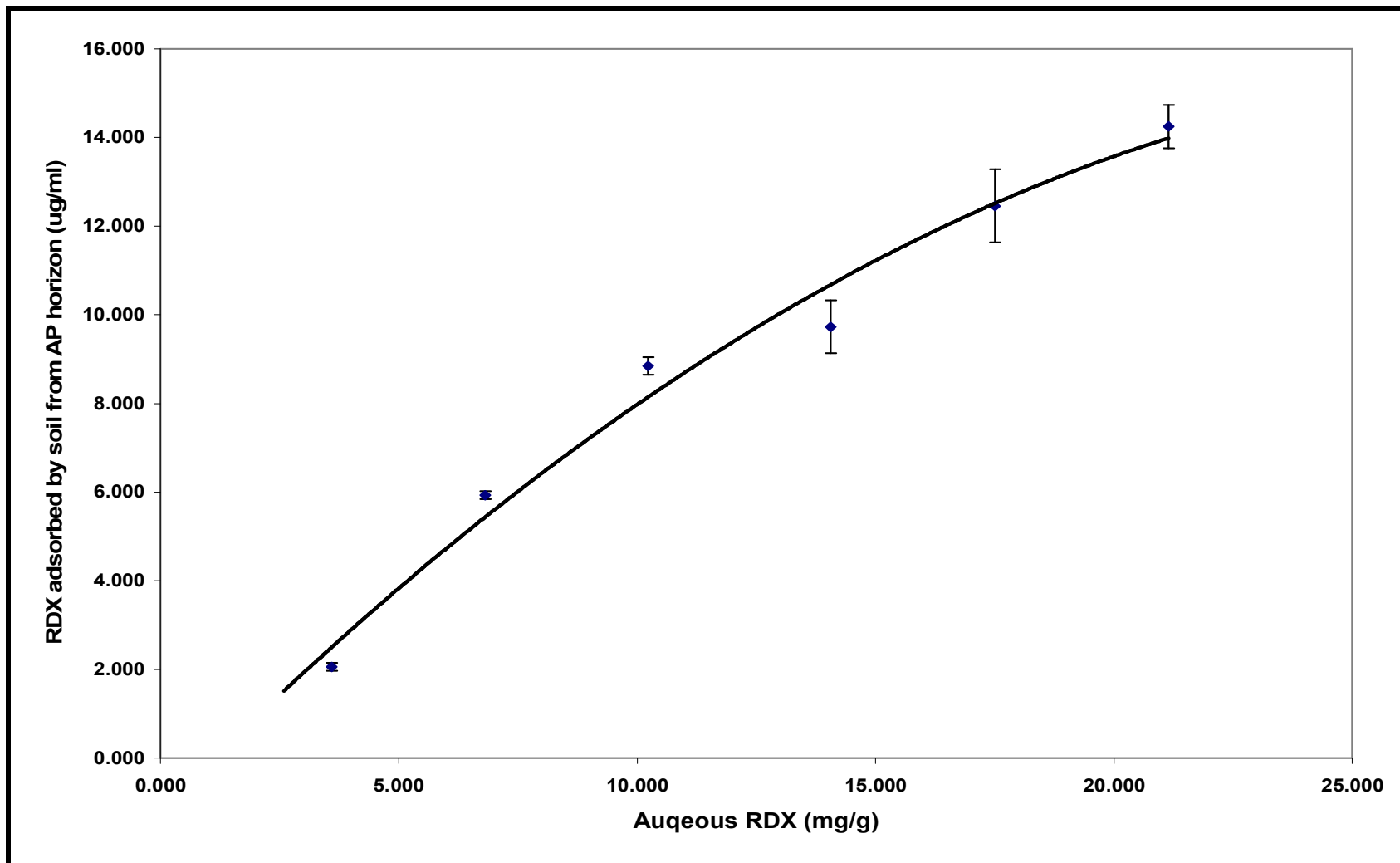


Figure A.1 Adsorption isotherm for RDX on soil from Ap horizon.

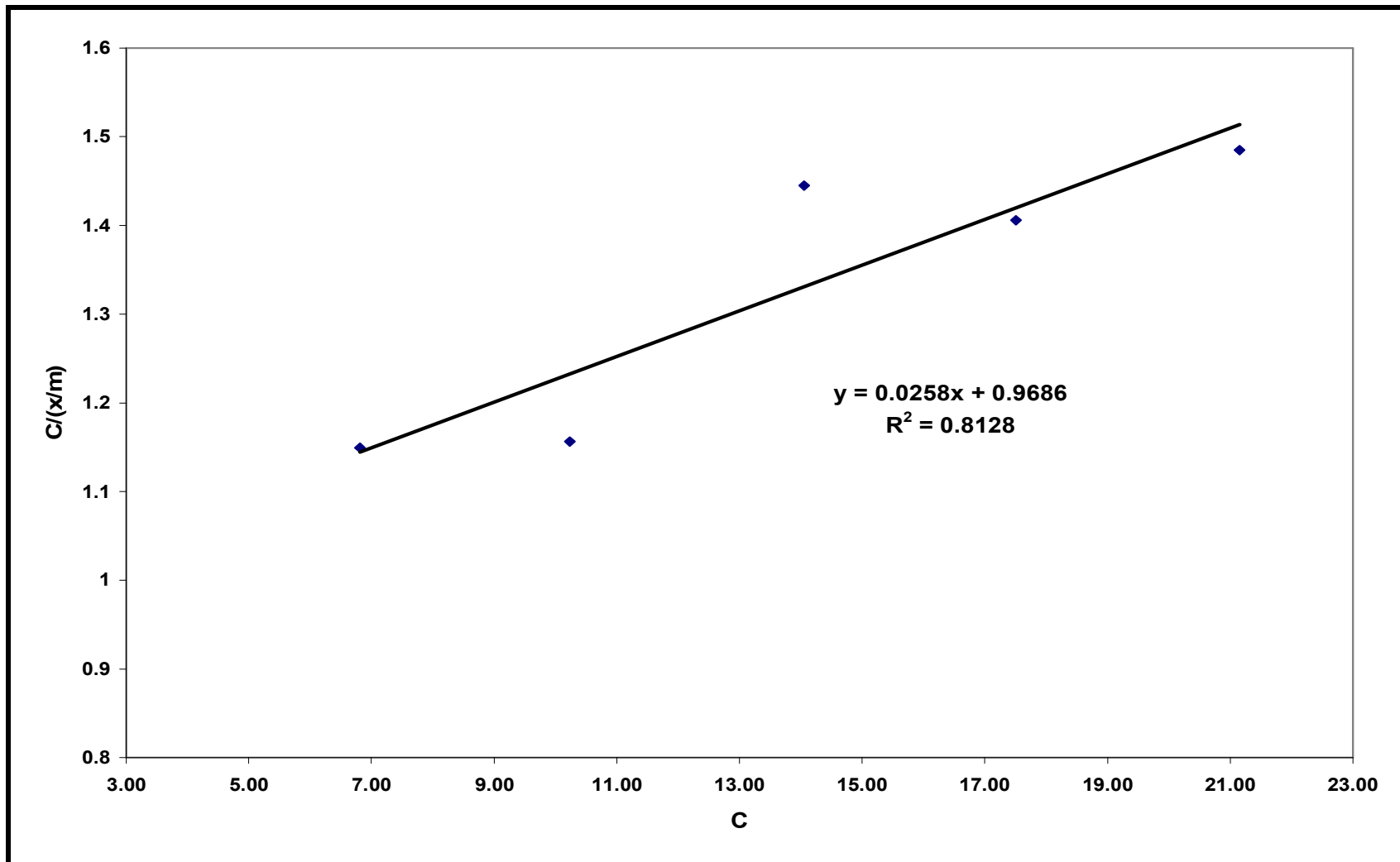


Figure A.2 Langmuir linear representation for RDX adsorption on soil from Ap horizon.

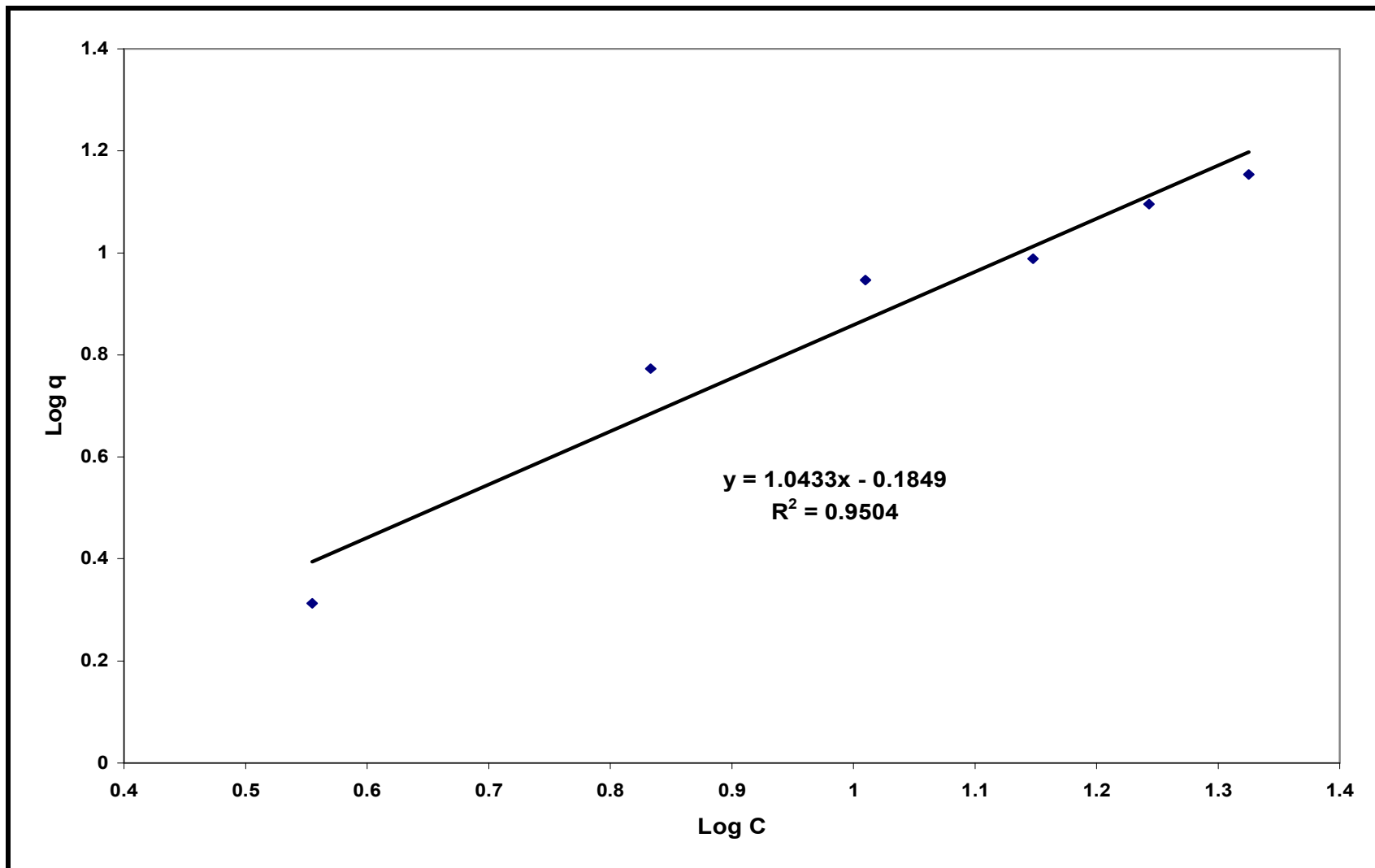


Figure A.3 Freundlich linear representation for RDX adsorption on soil from Ap horizon.

Table A.7 Experimental results for RDX interaction with soil from A horizon.

Sample ID	RDX Initial Concentration (ppm)	Area 1 (mAU)	Area 2 (mAU)	Average Area (mAU)	Concentration at equilibrium (ug/mL)	Mass in aqueous solution (ug)	Adsorbed mass (ug)	RDX adsorbed by topsoil (mg/kg)
1a	4.00	30.876	30.332	30.604	3.899	38.990	1.010	0.505
2a	8.00	56.168	56.244	56.206	7.515	75.146	4.854	2.427
3a	12.00	82.964	83.065	83.015	11.102	111.021	8.979	4.490
4a	16.00	113.499	113.707	113.603	15.195	151.954	8.046	4.023
5a	20.00	141.849	140.712	141.281	18.899	188.993	11.007	5.504
6a	24.00	168.337	167.912	168.125	22.492	224.915	15.085	7.542
Sample ID	RDX Initial Concentration (ppm)	Area 1 (mAU)	Area 2 (mAU)	Average Area (mAU)	Concentration at equilibrium (ug/mL)	Mass in aqueous solution (ug)	Adsorbed mass (ug)	RDX adsorbed by topsoil (mg/kg)
1b	4.00	30.667	30.711	30.689	3.910	39.100	0.900	0.450
2b	8.00	56.081	56.114	56.098	7.500	75.000	5.000	2.500
3b	12.00	83.778	83.575	83.677	11.191	111.907	8.093	4.047
4b	16.00	114.643	114.274	114.459	15.310	153.099	6.901	3.450
5b	20.00	140.972	140.920	140.946	18.854	188.545	11.455	5.728
6b	24.00	169.49	170.059	169.775	22.712	227.123	12.877	6.438
Sample ID	RDX Initial Concentration (ppm)	Area 1 (mAU)	Area 2 (mAU)	Average Area (mAU)	Concentration at equilibrium (ug/mL)	Mass in aqueous solution (ug)	Adsorbed mass (ug)	RDX adsorbed by topsoil (mg/kg)
1c	4.00	30.774	30.965	30.870	3.933	39.330	0.670	0.335
2c	8.00	56.351	56.568	56.460	7.548	75.485	4.515	2.258
3c	12.00	81.76	81.830	81.795	10.939	109.389	10.611	5.306
4c	16.00	114.149	114.746	114.448	15.308	153.085	6.915	3.458
5c	20.00	140.411	140.352	140.382	18.779	187.790	12.210	6.105
6c	24.00	169.072	168.461	168.767	22.577	225.774	14.226	7.113

Table A.8 RDX concentrations at equilibrium for three replicates, average concentration, and standard deviation for RDX interactions with soil from A horizon.

Concentration at equilibrium (ug/mL)	Concentration at equilibrium (ug/mL)	Concentration at equilibrium (ug/mL)	Average Concentration at equilibrium (ug/mL)	Standard Deviation
3.899	3.910	3.933	3.914	0.017
7.515	7.500	7.548	7.521	0.025
11.102	11.191	10.939	11.077	0.128
15.195	15.310	15.308	15.271	0.066
18.899	18.854	18.779	18.844	0.061
22.492	22.712	22.577	22.594	0.111

Table A.9 Adsorption of RDX by soil for three replicates, average adsorption, and standard deviation for RDX interactions with soil from A horizon.

RDX adsorbed by topsoil (mg/kg)	RDX adsorbed by topsoil (mg/kg)	RDX adsorbed by topsoil (mg/kg)	Average RDX adsorbed by topsoil (mg/kg)	Standard Deviation
0.505	0.450	0.335	0.430	0.087
2.427	2.500	2.258	2.395	0.124
4.490	4.047	5.306	4.614	0.639
4.023	3.450	3.458	3.644	0.329
5.504	5.728	6.105	5.779	0.304
7.542	6.438	7.113	7.031	0.557

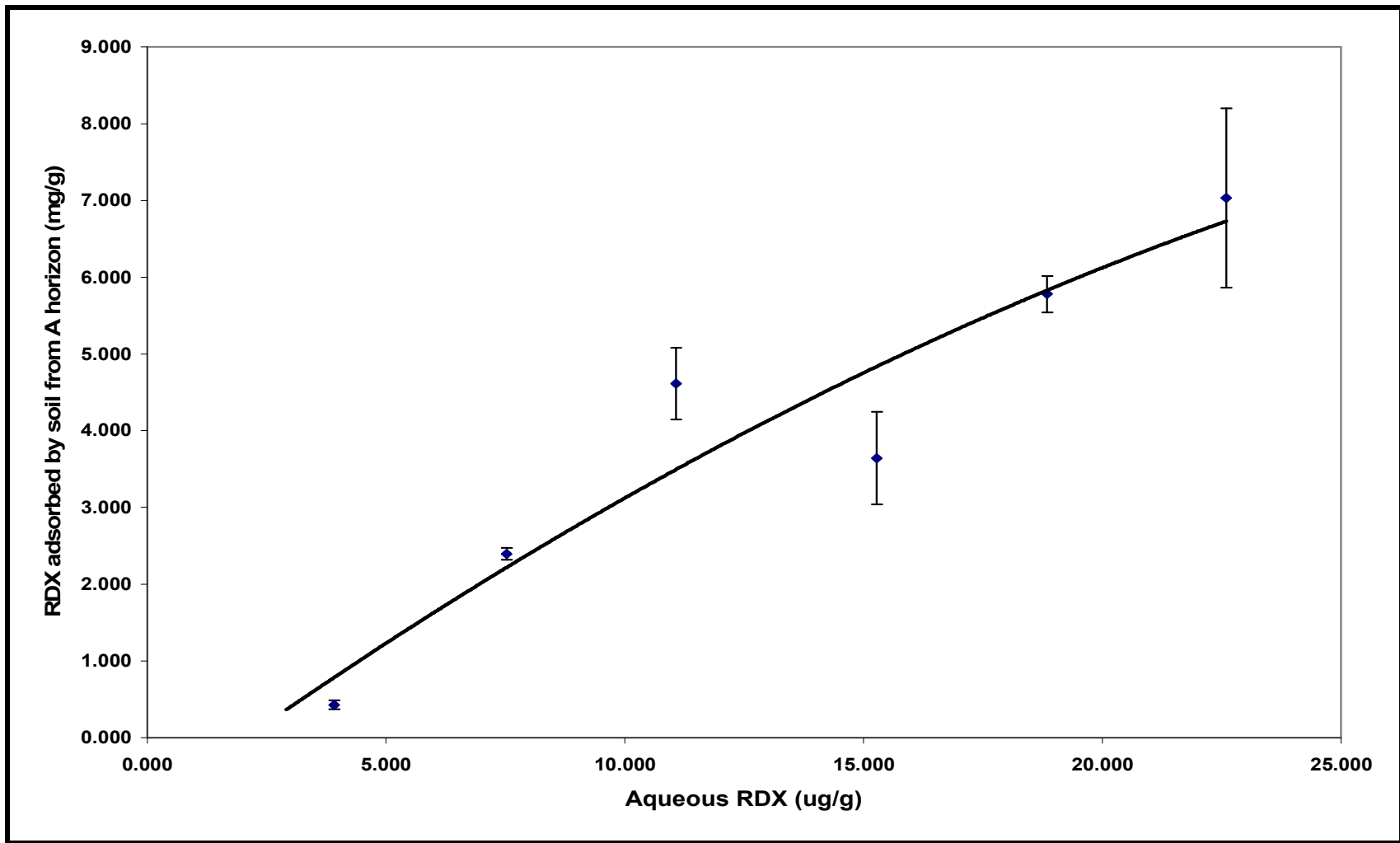


Figure A.4 Adsorption isotherm for RDX on soil from A horizon.

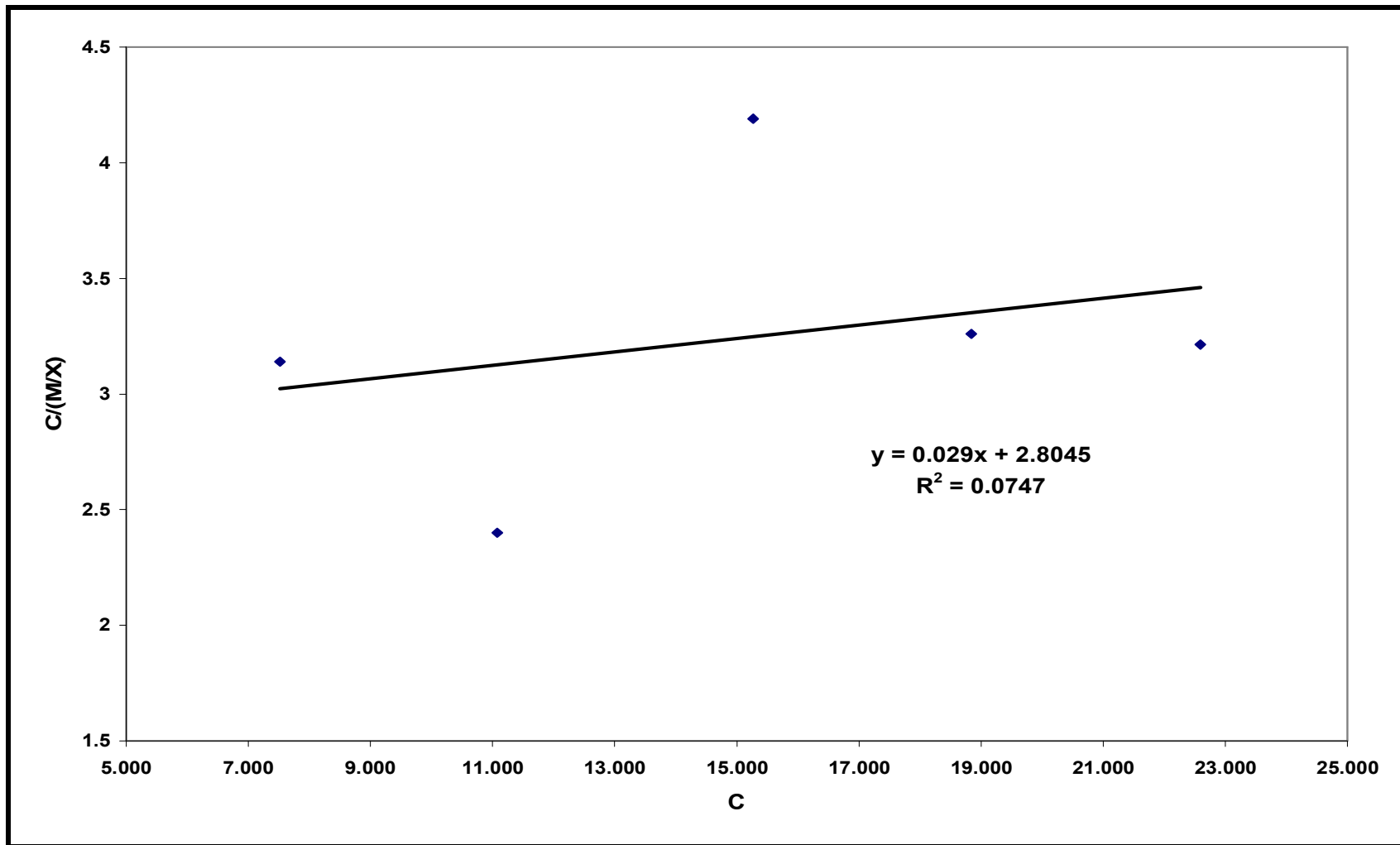


Figure A.5 Langmuir linear representation for RDX adsorption on soil from A horizon.

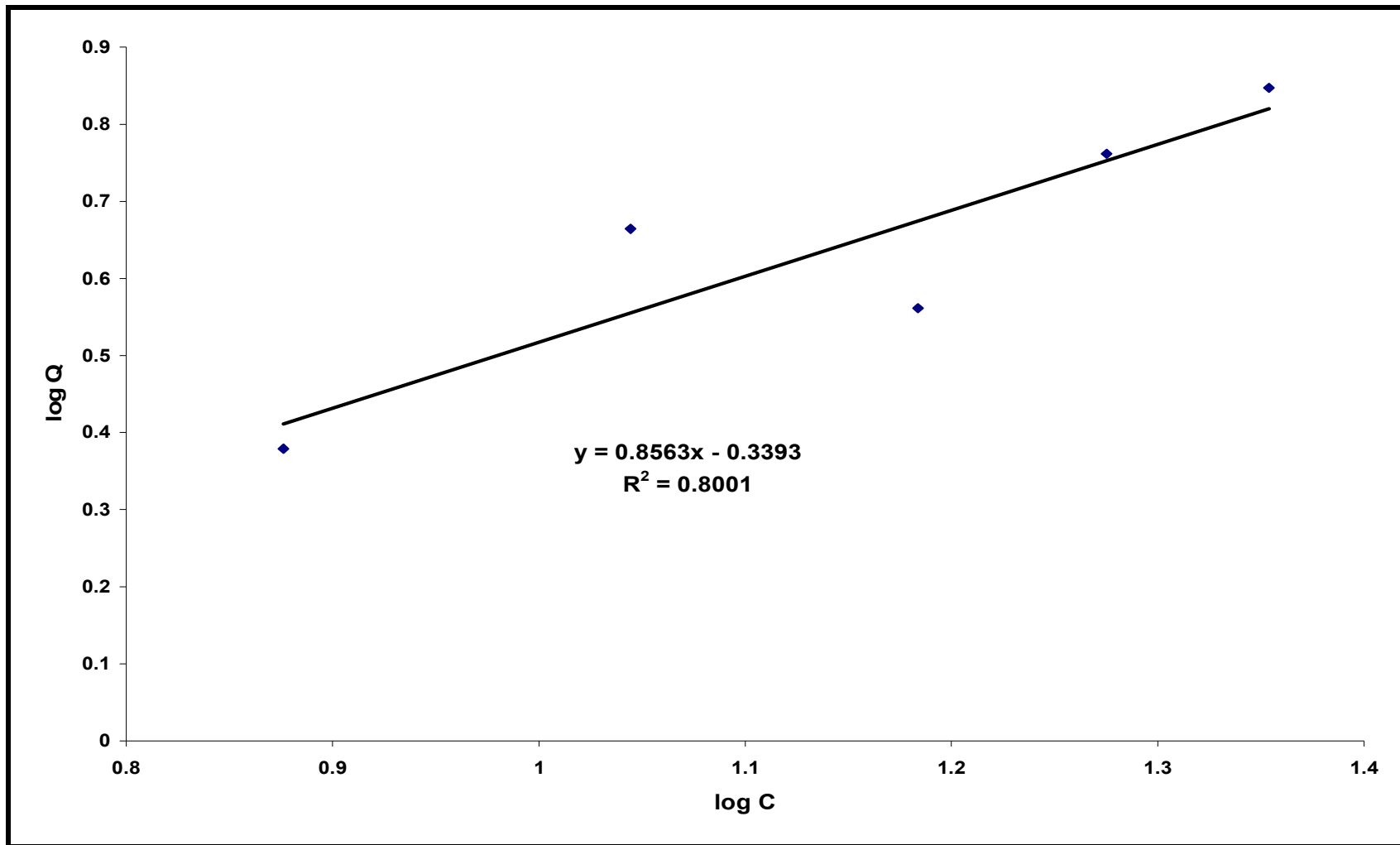


Figure A.6 Freundlich linear representation for RDX adsorption on soil from A horizon.

Table A.10 Experimental results for RDX interaction with the clay fraction from A horizon.

Sample ID	Area 1 (mAU)	Area 2 (mAU)	Average Area (mAU)	Concentration at equilibrium (ug/mL)	Mass in aqueous solution (ug)	Adsorbed mass (ug)	RDX adsorbed by clay fraction (mg/kg)
1a	31.781	31.702	31.742	3.792	37.916	2.084	10.421
2a	62.278	62.195	62.237	7.751	77.507	2.493	12.463
3a	89.750	89.614	89.682	11.643	116.434	3.566	17.829
4a	122.570	122.610	122.590	15.586	155.864	4.136	20.678
5a	151.896	151.902	151.899	19.392	193.916	6.084	30.418
6a	183.153	183.145	183.149	23.449	234.488	5.512	27.559

Sample ID	Area 1 (mAU)	Area 2 (mAU)	Average Area (mAU)	Concentration at equilibrium (ug/mL)	Mass in aqueous solution (ug)	Adsorbed mass (ug)	RDX adsorbed by clay fraction (mg/kg)
1a	31.692	31.752	31.722	3.789	37.890	2.110	10.548
2a	62.592	62.656	62.624	7.801	78.011	1.989	9.947
3a	89.152	89.085	89.119	11.570	115.703	4.297	21.487
4a	122.850	122.912	122.881	15.624	156.242	3.758	18.789
5a	152.608	152.545	152.577	19.480	194.796	5.204	26.020
6a	183.472	183.650	183.561	23.502	235.023	4.977	24.884

Sample ID	Area 1 (mAU)	Area 2 (mAU)	Average Area (mAU)	Concentration at equilibrium (ug/mL)	Mass in aqueous solution (ug)	Adsorbed mass (ug)	RDX adsorbed by clay fraction (mg/kg)
1a	31.856	31.901	31.879	3.809	38.094	1.906	9.532
2a	62.02	62.268	62.144	7.739	77.387	2.613	13.063
3a	89.410	89.502	89.456	11.614	116.141	3.859	19.296
4a	122.356	122.692	122.524	15.578	155.779	4.221	21.106
5a	152.985	152.973	152.979	19.532	195.319	4.681	23.407
6a	183.705	183.802	183.754	23.527	235.273	4.727	23.634

Table A.11 RDX concentrations at equilibrium for three replicates, average concentration, and standard deviation for RDX interaction with the clay fraction from A horizon.

Concentration at equilibrium (ug/mL)	Concentration at equilibrium (ug/mL)	Concentration at equilibrium (ug/mL)	Average concentration at equilibrium (ug/mL)	Standard Deviation
3.792	3.789	3.809	3.797	0.011
7.751	7.801	7.739	7.764	0.033
11.643	11.570	11.614	11.609	0.037
15.586	15.624	15.578	15.596	0.025
19.392	19.480	19.532	19.468	0.071
23.449	23.502	23.527	23.493	0.040

Table A.12 Adsorption of RDX by clay fraction for three replicates, average adsorption, and standard deviation for RDX interactions with the clay fraction from A horizon.

RDX adsorbed by clay fraction (mg/kg)	RDX adsorbed by clay fraction (mg/kg)	RDX adsorbed by clay fraction (mg/kg)	Average RDX adsorbed by clay fraction (mg/kg)	Standard Deviation
10.421	10.548	9.532	10.167	0.554
12.463	9.947	13.063	11.824	1.653
17.829	21.487	19.296	19.537	1.841
20.678	18.789	21.106	20.191	1.233
30.418	26.020	23.407	26.615	3.543
27.559	24.884	23.634	25.359	2.005

Table A.13 Experimental results for RDX interaction with the clay fraction from Ap horizon.

Sample ID	RDX Initial Concentration (TNT)	Area 1 (mAU)	Area 2 (mAU)	Average Area (mAU)	Concentration at equilibrium (ug/mL)	Mass in aqueous solution (ug)	Adsorbed mass (ug)	RDX adsorbed by clay fraction (mg/kg)
1a	4.00	31.985	31.802	31.894	3.811	38.113	1.887	9.434
2a	8.00	62.629	62.525	62.577	7.795	77.950	2.050	10.252
3a	12.00	89.926	89.885	89.906	11.672	116.724	3.276	16.378
4a	16.00	123.255	123.118	123.187	15.664	156.639	3.361	16.805
5a	20.00	152.995	152.899	152.947	19.528	195.277	4.723	23.615
6a	24.00	183.908	183.778	183.843	23.539	235.389	4.611	23.053
Sample ID	RDX Initial Concentration (TNT)	Area 1 (mAU)	Area 2 (mAU)	Average Area (mAU)	Concentration at equilibrium (ug/mL)	Mass in aqueous solution (ug)	Adsorbed mass (ug)	RDX adsorbed by clay fraction (mg/kg)
1b	4.00	31.505	31.489	31.497	3.760	37.598	2.402	12.008
2b	8.00	62.265	62.320	62.293	7.758	77.580	2.420	12.099
3b	12.00	90.043	90.112	90.078	11.695	116.948	3.052	15.262
4b	16.00	123.525	123.608	123.567	15.713	157.132	2.868	14.339
5b	20.00	153.203	153.115	153.159	19.555	195.552	4.448	22.239
6b	24.00	183.886	183.956	183.921	23.549	235.491	4.509	22.547
Sample ID	RDX Initial Concentration (TNT)	Area 1 (mAU)	Area 2 (mAU)	Average Area (mAU)	Concentration at equilibrium (ug/mL)	Mass in aqueous solution (ug)	Adsorbed mass (ug)	RDX adsorbed by clay fraction (mg/kg)
1c	4.00	32.556	32.554	32.555	3.897	38.972	1.028	5.140
2c	8.00	62.412	62.530	62.471	7.781	77.812	2.188	10.940
3c	12.00	89.805	90.137	89.971	11.681	116.809	3.191	15.953
4c	16.00	123.08	123.092	123.086	15.651	156.508	3.492	17.458
5c	20.00	153.202	153.180	153.191	19.559	195.594	4.406	22.031
6c	24.00	183.808	184.046	183.927	23.550	235.498	4.502	22.508

Table A.14 RDX concentrations at equilibrium for three replicates, average concentration, and standard deviation for RDX interaction with the clay fraction from Ap horizon.

Concentration at equilibrium (ug/mL)	Concentration at equilibrium (ug/mL)	Concentration at equilibrium (ug/mL)	Average concentration at equilibrium (ug/mL)	Standard Deviation
3.811	3.760	3.897	3.823	0.069
7.795	7.758	7.781	7.778	0.019
11.672	11.695	11.681	11.683	0.012
15.664	15.713	15.651	15.676	0.033
19.528	19.555	19.559	19.547	0.017
23.539	23.549	23.550	23.546	0.006

Table A.15 Adsorption of RDX by clay fraction for three replicates, average adsorption, and standard deviation for RDX interactions with the clay fraction from A horizon.

RDX adsorbed by clay fraction (mg/kg)	RDX adsorbed by clay fraction (mg/kg)	RDX adsorbed by clay fraction (mg/kg)	Average RDX adsorbed by clay fraction (mg/kg)	Standard Deviation
9.434	12.008	5.140	8.861	3.470
10.252	12.099	10.940	11.097	0.933
16.378	15.262	15.953	15.864	0.563
16.805	14.339	17.458	16.201	1.645
23.615	22.239	22.031	22.628	0.861
23.053	22.547	22.508	22.703	0.304

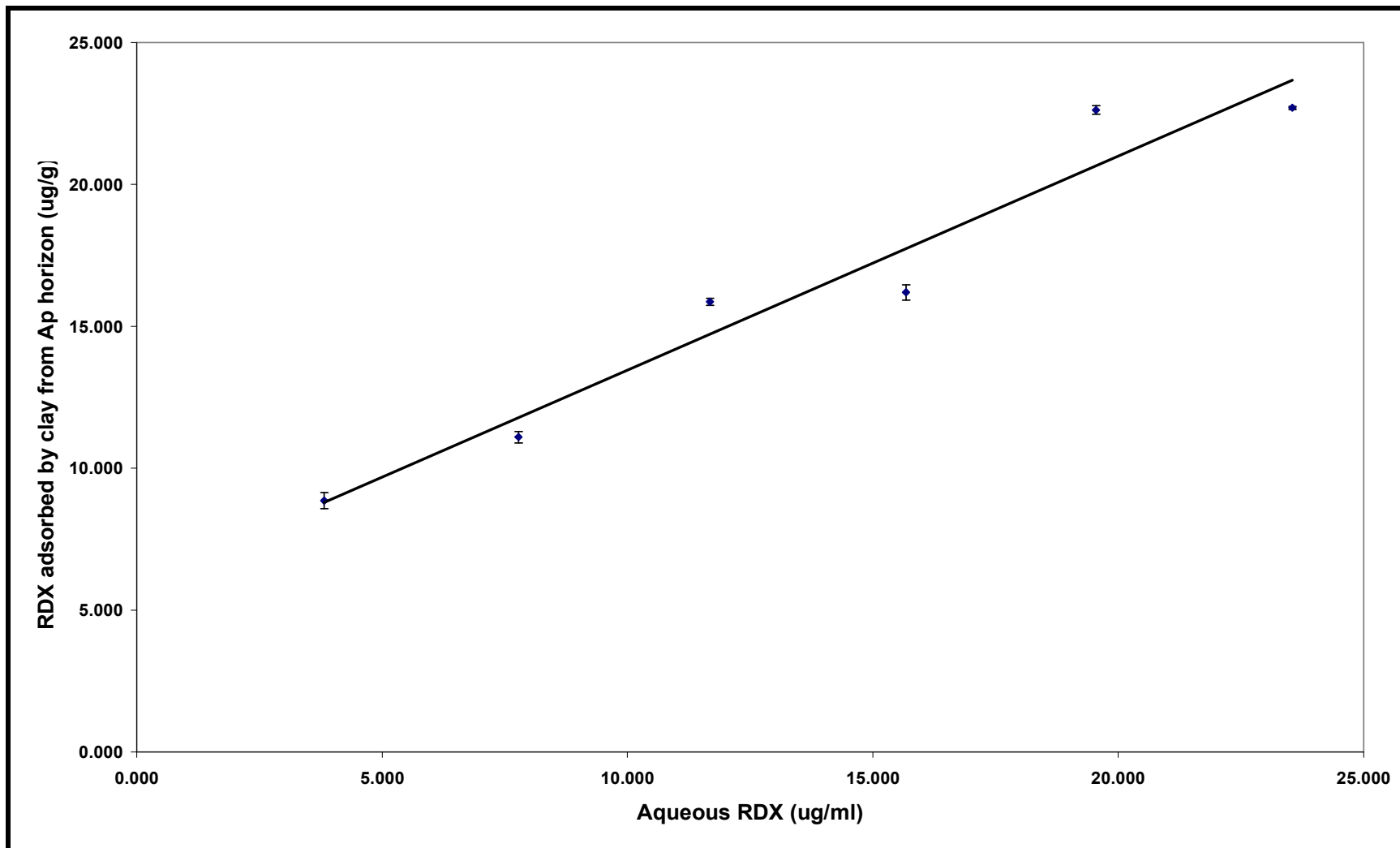


Figure A.7 Adsorption isotherm for RDX on clay from Ap horizon.

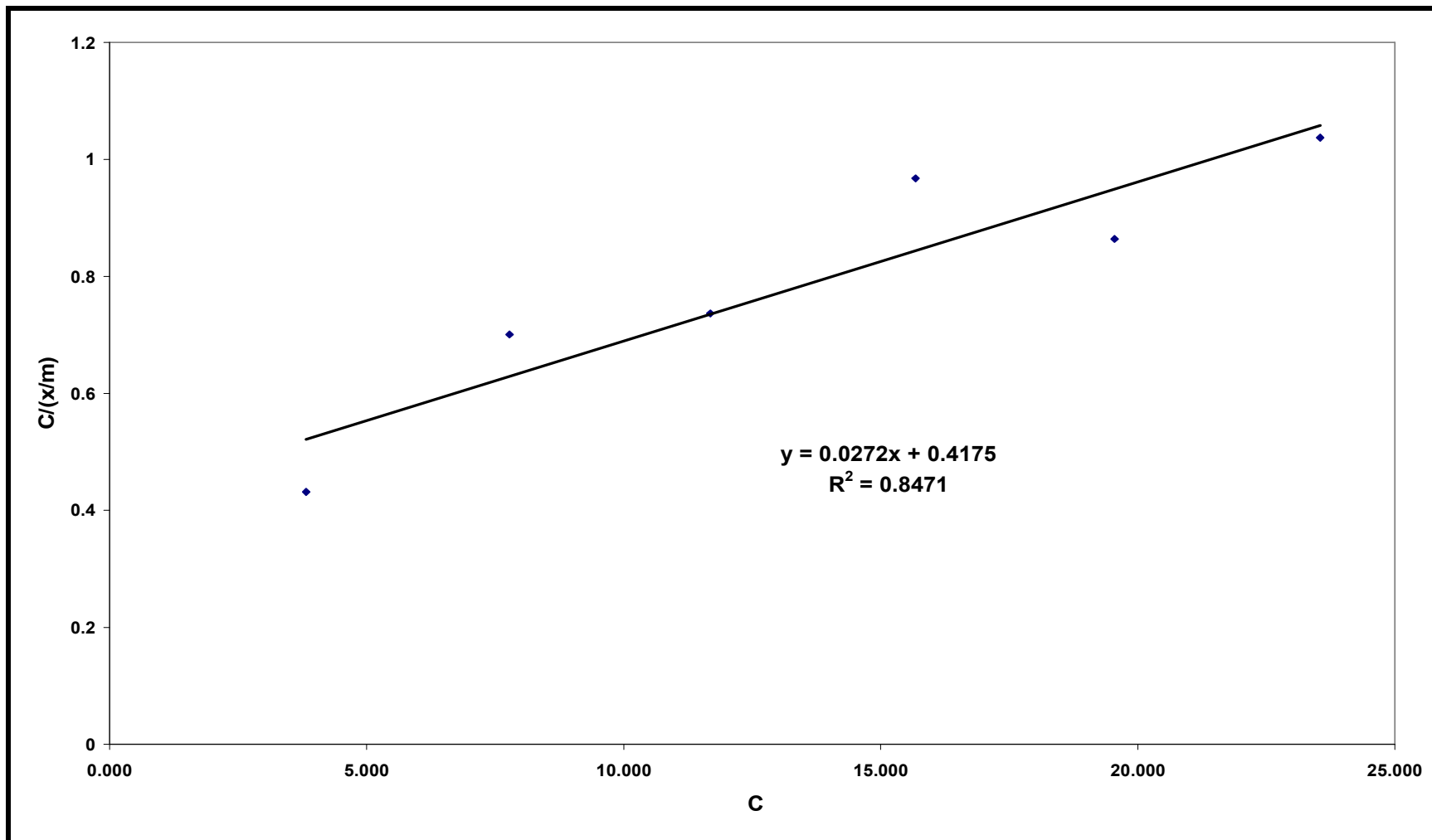


Figure A.8 Langmuir linear representation for RDX adsorption on clay from Ap horizon.

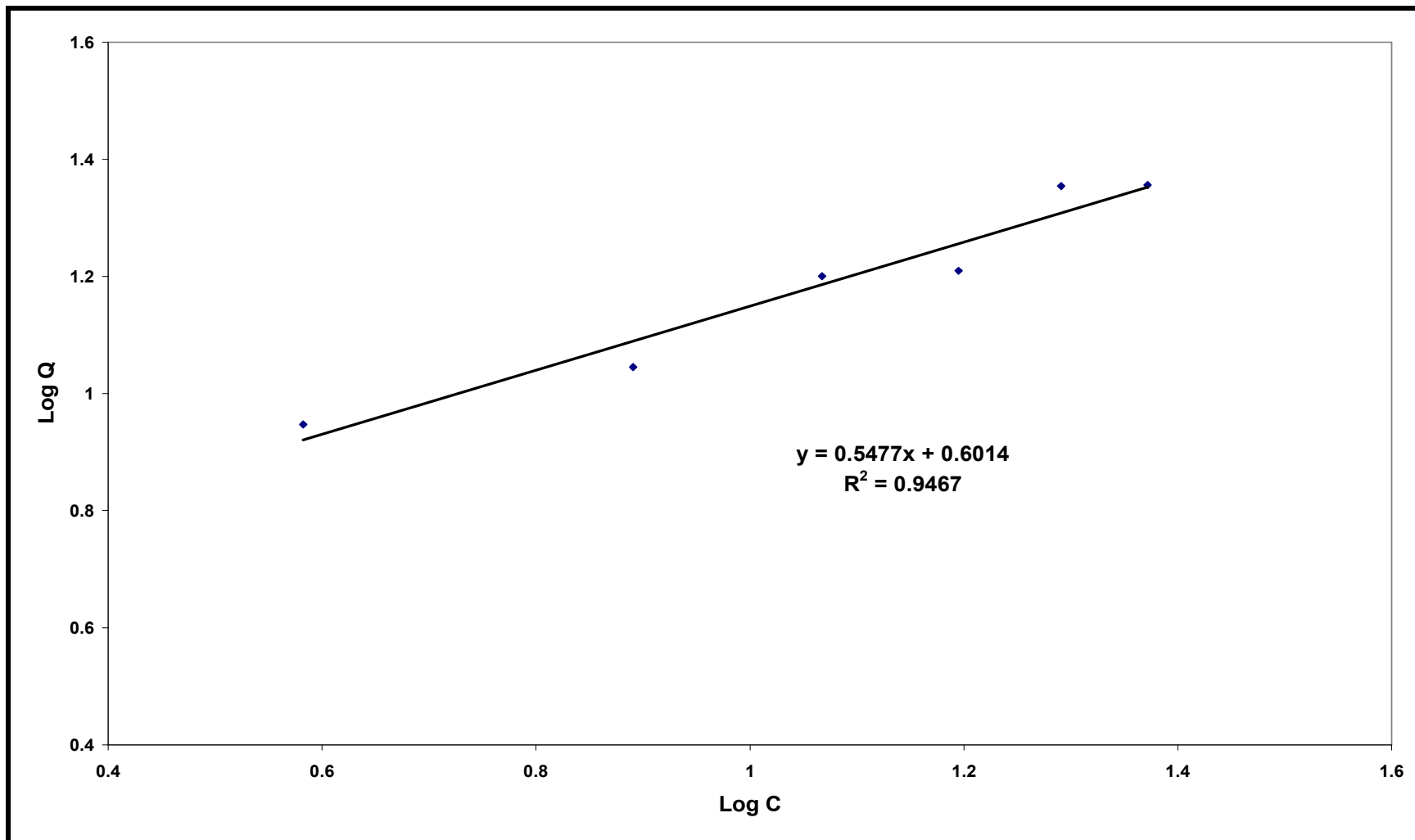


Figure A.9 Freundlich linear representation for RDX adsorption on clay from Ap horizon.

Table A.16 Experimental results for RDX interaction with the clay fraction from UPRM.

Sample ID	RDX Initial Concentration (TNT)	Area 1 (mAU)	Area 2 (mAU)	Average Area (mAU)	Concentration at equilibrium (ug/mL)	Mass in aqueous solution (ug)	Adsorbed mass (ug)	RDX adsorbed by clay fraction (mg/kg)
1a	4.00	32.253	32.200	32.227	3.855	38.545	1.455	7.273
2a	8.00	62.881	62.902	62.892	7.836	78.358	1.642	8.211
3a	12.00	90.422	90.526	90.474	11.746	117.462	2.538	12.688
4a	16.00	123.415	123.388	123.402	15.692	156.918	3.082	15.410
5a	20.00	154.118	154.025	154.072	19.674	196.737	3.263	16.315
6a	24.00	181.998	182.194	182.096	23.642	236.415	3.585	17.923
Sample ID	RDX Initial Concentration (TNT)	Area 1 (mAU)	Area 2 (mAU)	Average Area (mAU)	Concentration at equilibrium (ug/mL)	Mass in aqueous solution (ug)	Adsorbed mass (ug)	RDX adsorbed by clay fraction (mg/kg)
1b	31.983	31.852	31.918	31.918	3.814	38.144	1.856	9.279
2b	62.998	63.012	63.005	63.005	7.851	78.505	1.495	7.474
3b	89.855	89.959	89.907	89.907	11.673	116.726	3.274	16.368
4b	123.155	123.085	123.120	123.120	15.655	156.553	3.447	17.237
5b	153.705	153.519	153.612	153.612	19.614	196.140	3.860	19.298
6b	182.405	182.201	182.303	182.303	23.668	236.684	3.316	16.579
Sample ID	RDX Initial Concentration (TNT)	Area 1 (mAU)	Area 2 (mAU)	Average Area (mAU)	Concentration at equilibrium (ug/mL)	Mass in aqueous solution (ug)	Adsorbed mass (ug)	RDX adsorbed by clay fraction (mg/kg)
1c	4.00	32.175	32.373	32.274	3.785	37.850	2.150	10.750
2c	8.00	62.755	62.802	62.779	7.821	78.211	1.789	8.944
3c	12.00	90.881	90.985	90.933	11.806	118.058	1.942	9.708
4c	16.00	123.705	123.969	123.837	15.748	157.483	2.517	12.583
5c	20.00	154.752	154.612	154.682	19.753	197.530	2.470	12.352
6c	24.00	182.325	182.455	182.390	23.680	236.797	3.203	16.015

Table A.17 RDX concentrations at equilibrium for three replicates, average concentration, and standard deviation for RDX interaction with the clay fraction from UPRM.

Concentration at equilibrium (ug/mL)	Concentration at equilibrium (ug/mL)	Concentration at equilibrium (ug/mL)	Average concentration at equilibrium (ug/mL)	Standard Deviation
3.855	3.814	3.785	3.843	0.035
7.836	7.851	7.821	7.836	0.015
11.746	11.673	11.806	11.742	0.067
15.692	15.655	15.748	15.698	0.047
19.674	19.614	19.753	19.680	0.070
23.642	23.668	23.680	23.663	0.019

Table A.18 Adsorption of RDX by clay fraction for three replicates, average adsorption, and standard deviation for RDX interactions with the clay fraction from A horizon.

RDX adsorbed by clay fraction (mg/kg)	RDX adsorbed by clay fraction (mg/kg)	RDX adsorbed by clay fraction (mg/kg)	Average RDX adsorbed by clay fraction (mg/kg)	Standard Deviation
7.273	9.279	10.750	9.101	1.745
8.211	7.474	8.944	8.210	0.735
12.688	16.368	9.708	12.921	3.336
15.410	17.237	12.583	15.077	2.345
16.315	19.298	12.352	15.988	3.485
17.923	16.579	16.015	16.839	0.980

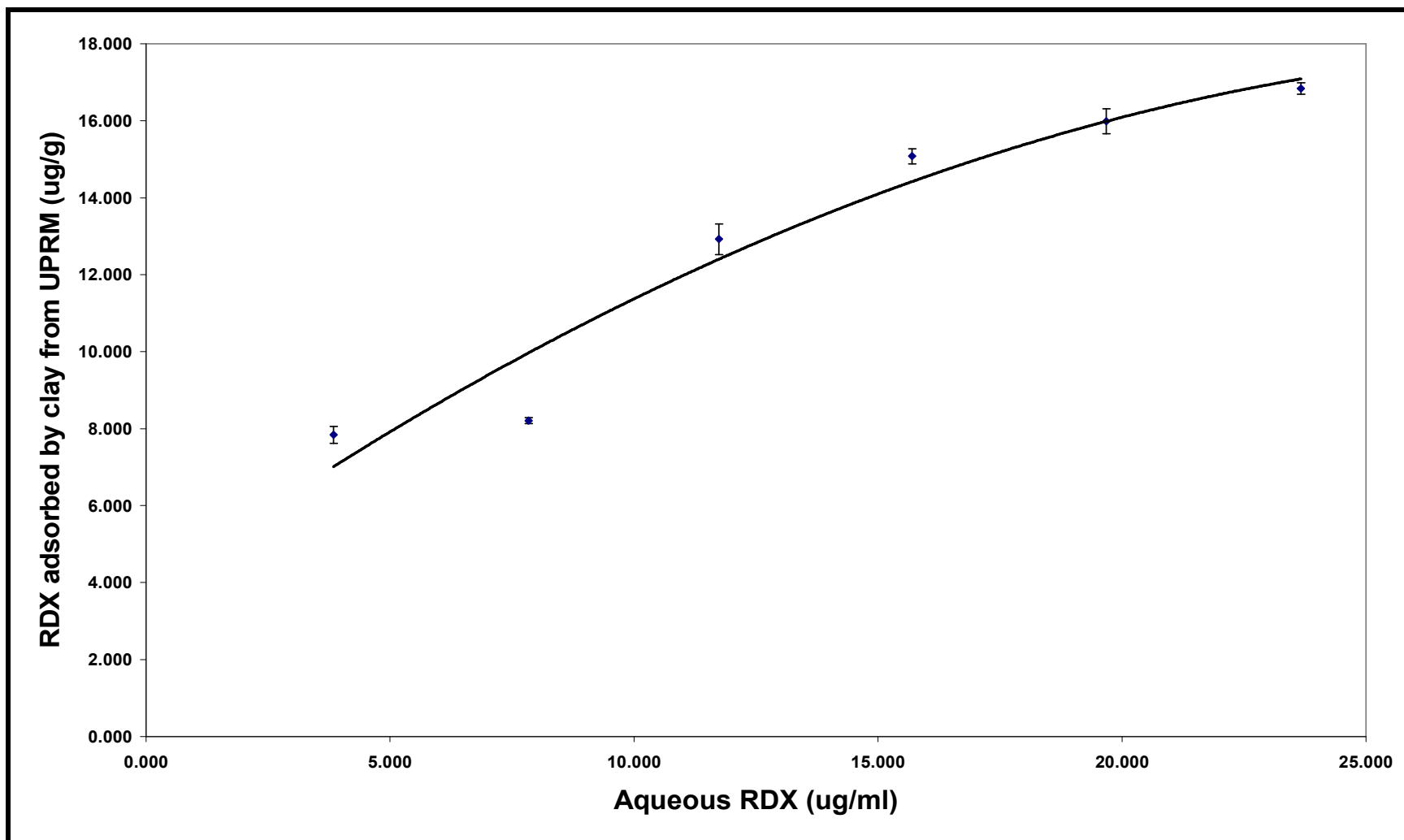


Figure A.10 Adsorption isotherm for RDX on clay from UPRM.

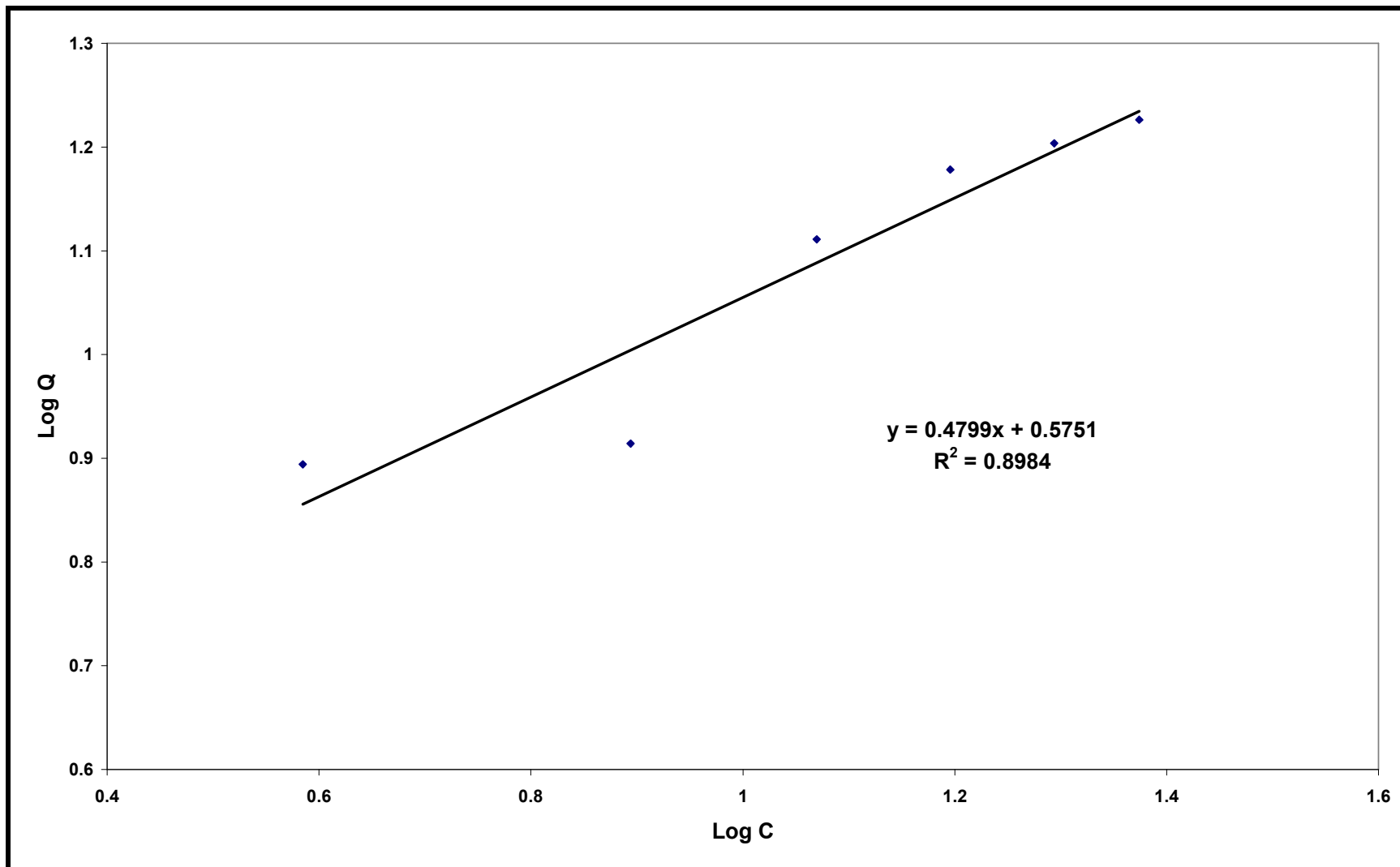


Figure A.11 Freundlich linear representation for RDX adsorption on clay from UPRM.

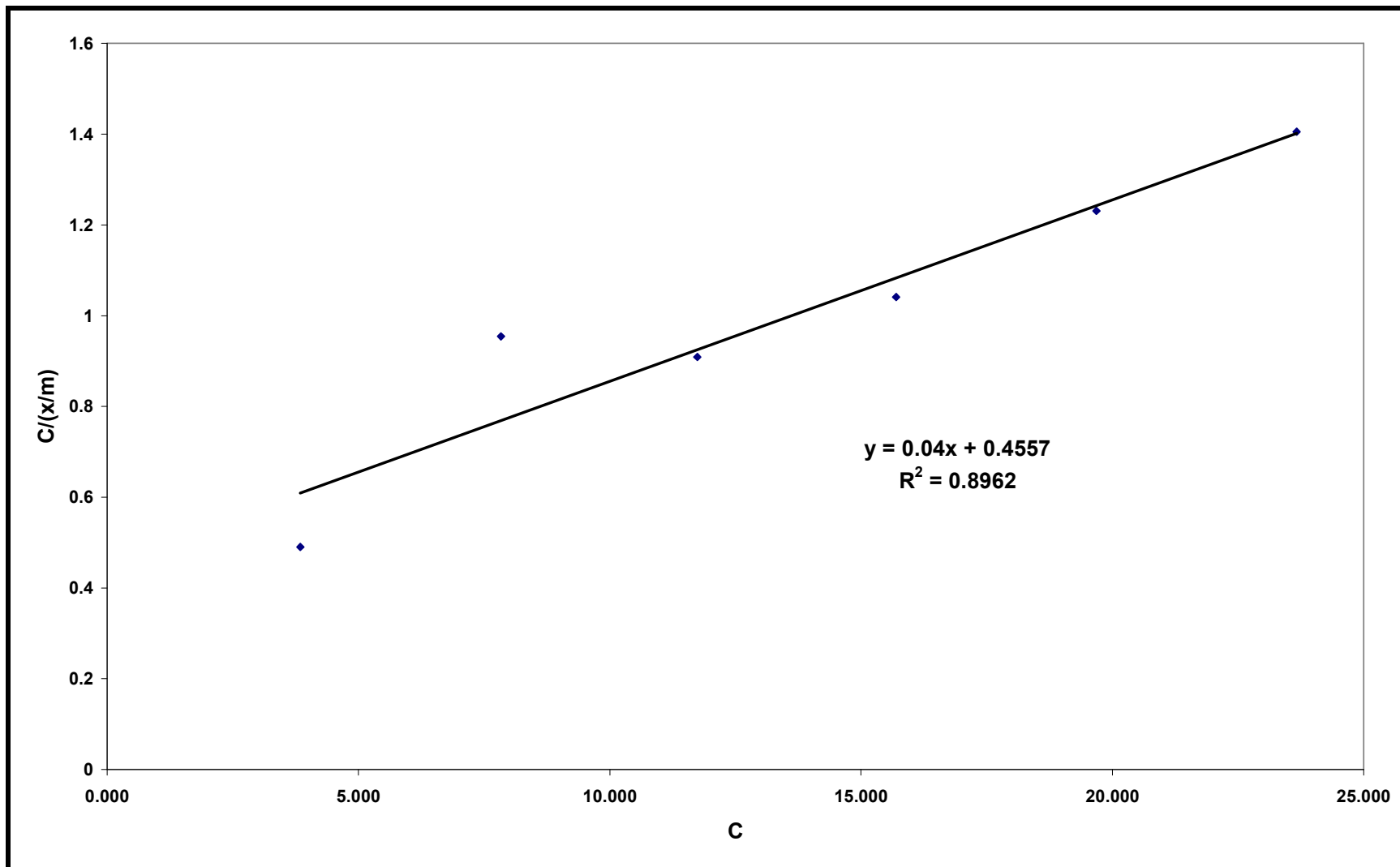


Figure A.12 Langmuir linear representation for RDX adsorption on clay from UPRM